November 2016
Volume 122
Issue 1967
£5.60

www.electronicsworld.co.uk

Electronics WORLD

THE ESSENTIAL ELECTRONICS ENGINEERING MAGAZINE

SPECIAL REPORT

CONSUMER ELECTRONICS DESIGN

- Charging and power management
- Security and eco-friendliness
- Protection and waterproofing

HD 1024

10-Bit HD Oscilloscopes

Provide Exceptional Signal Fidelity Up To 4GHz and 40GS/s

TELEDYNE LECROY

Technology
New test to help commercialise printable electronics

Embedded Design
Ultraviolet sensors in embedded applications

Products
Replacement for obsolete and end-of-life tape drives

38

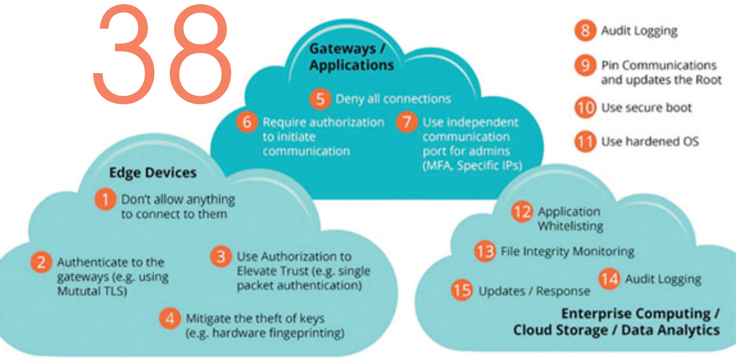

REGULARS

Cover supplied by
TELEDYNE LECROY
More on pages 8-9

30

FEATURES

BATTERY INNOVATION IS ALIVE AND WELL IN THE UK

Did you know that it was the British chemist Joseph Swan who invented the lightbulb? While Thomas Edison frequently receives the praise for the lightbulb moment, it was Swan who first developed the incandescent bulb and lit his house with electricity. This is one of many great contributions that the UK has made to the field of science and technology, with the industry showing little signs of slowing down.

If you believe the fears of critics in the engineering and manufacturing sector, you likely believe the UK is falling behind in the technical arms race. This simply is not the case. The UK remains one of the world's leading countries for technology, producing the second most cited research papers in the world, as well as providing a surprisingly thriving landscape for development.

We need to look no further than the battery sector to confirm this. While many countries turn their attentions to more glamorous technical fields such as robotics, UK original equipment manufacturers (OEMs) in the battery sector continue to make improvements in the way we power the future.

For example, a number of promising new proposals for battery technologies, such as sodium-ion and unlikely chemistries such as copper-foam, have emerged from the UK in recent years. This is only possible due to the battery research funding that is available in the country, such as the government's Innovate UK research grant, among others.

The Innovate UK grant has previously been awarded to a start-up battery OEM for its research into sodium-ion technologies. These batteries would be used in electric vehicles, a rapidly expanding market in the UK. In fact, electric vehicles currently represent 1.4% of all new car registrations in the country in 2016, with an average of 3,000 sold per month between January and May 2016. This is driving a need for high-performance vehicle batteries.

Of course, the humble lithium-ion (Li-ion) battery doesn't get lost in all the excitement. OEMs in the UK are working to ensure that this staple of modern power is able to keep up with the demands and challenges presented by a rapidly changing industry.

At Accutronics, for example, developers have identified growing concerns over battery counterfeiting compromising electronic devices and making them unreliable. To tackle this problem, Accutronics

> "While many countries turn their attentions to more glamorous technical fields, UK OEMs in the battery sector that continue to make improvements in the way we power the future

introduced secure hashing algorithm encryption, known as algorithmic security, into its batteries as well as into the medical devices they power, so that fake batteries are rejected by the device.

Recently, the Engineering and Physical Sciences Research Council (EPSRC) provided a £6.8m grant to a team to develop next-generation lithium batteries. This was fuelled by the recent widespread uptake of portable and wearable electronics, a technology trend that has stretched from the consumer to the commercial sector to professional industries such as medical technology (medtech).

The trend for portable and wearable devices was recently reflected in the National Health Service's (NHS's) new nationwide system for purchasing medical devices, including implantable defibrillators. Implantable electronics such as these present the challenge of delivering adequate battery life from a primary, non-rechargeable cell.

Authors in the British Medical Journal (BMJ) also highlighted this problem, arguing that the battery life of implantable medical devices (IMDs) needs to be longer to avoid the frequent surgery currently required and the subsequent risk of infection.

Careful consideration of battery chemistry and power discharge characteristics, as well as the ease of charging should be at the top of design engineers' lists when embarking on a new project.

Combining this with smart battery features such as accurate charge gauging, as well as continued innovation into new materials, it is not beyond reason to hope that UK OEMs make the next great scientific contribution, leading to the next great lightbulb moment.

Michele Windsor is Sales and Marketing Manager at Accutronics (www.accutronics.co.uk)

EDITOR:
Svetlana Josifovska
Tel: +44 (0)1732 883392
Email: svetlanaj@sjpbusinessmedia.com

SALES:
James Corner
Tel: +44 (0)20 7933 8985
Email: jamesc@electronicsworld.co.uk

Philip Woolley
Tel: +44 (0)20 7933 8989
Email: philipw@sjpbusinessmedia.com

DESIGN: Tania King

PUBLISHER: Wayne Darroch
ISSN: 1365-4675

PRINTER: Buxton Press Ltd

SUBSCRIPTIONS:
Subscription rates:
1 year: £65 (UK); £94 (worldwide)
Tel/Fax +44 (0)1635 879361/868594
Email: electronicsworld@circdata.com
www.electronicsworld.co.uk/subscribe

SJP business media
2nd Floor,
52-54 Gracechurch Street,
London, EC3V 0EH

Follow us on Twitter
@electrowo

Join us on LinkedIn

ALTERNATIVE BATTERY SYSTEM GIVES ELECTRIC CARS INDEPENDENCE FROM CHARGING STATIONS

Future electric cars won't need to wait to charge at stations thanks to a set of easily replaceable battery modules, located on the side of the car

The City eTaxi is one of the first electric vehicles on the road to operate completely independent of either existing or future charging stations, thanks to a battery system developed by lithium-ion battery producer BMZ.

The City eTaxi is driven by two hub motors, powered by six single battery modules connected by an intelligent battery management system. With battery capacity of 1.9kWh each, the six-pack enables driving distance of some 120km and acceleration to over 80km/h, if required.

The battery replacement system was developed so a driver can easily replace a single low voltage module when low on charge, without lengthy waiting at a re-charging station. All the driver needs to do is be authenticated at a special replacement station, which releases trays to swap the empty modules. The modules weigh some 15kg, and are safe and inactive when disconnected. BMZ envisages automatic replacements in the future, without driver involvement.

The City eTaxi is part of a larger e-mobility project in Germany called "Adaptive City Mobility 2 (ACM 2)", funded by the German Federal Ministry for Economic Affairs and Energy. The project aims to pave the way for lightweight electric cars in urban environments on a large scale.

NPL DEVELOPS A NEW TEST TO HELP COMMERCIALISE PRINTABLE ELECTRONICS

The UK's National Physical Laboratory (NPL) has developed a new, non-destructive method of measuring the three-dimensional orientation of molecules in organic semiconductor transistors, using Raman spectroscopy. This will create a new, faster and more flexible method of measuring electrical conductivity in a printed circuit.

Modern electronic devices, such as LEDs or solar cells, can save significant cost and weight by using organic semiconductors, which enable large-volume printing of electronic circuits onto thin sheets of plastic. The ink consists of organic polymer molecules that conduct electricity, but when dry they crystallise in all directions, preventing conductivity.

Measuring the direction of molecules in a printed circuit is a key part of the quality control process, but until now was impossible to do non-destructively and in 3D. NPL's new method takes advantage of how a molecule vibrates when light shines on it. Different vibrations change the frequency of the reflected light – the main principle behind Raman spectroscopy. Molecules facing different directions will vibrate differently as a laser is passed over, causing reflected light of different wavelengths. By measuring these different frequencies, NPL's test reveals the orientation of molecules in the circuit in 3D.

Current printable electronics mostly use inorganic, non-printed semiconductor components. A new test enables these components also to be printed

By creating such a test for printed electronic circuits, the efficiency of producing electronic devices can be drastically increased, leading to cheaper, faster and better-quality electronics.

HIROSE AND HARTING WORK ON A NEW 10GBIT ETHERNET CONNECTOR STANDARD

Tokyo-based Hirose Electric and Harting Electronics from Espelkamp, Germany, have agreed to jointly develop, standardise and commercialise a miniaturized connector system for 10Gbit Ethernet.

Ten years ago, the RJ45 ruled the Ethernet sphere, however nowadays is not completely suitable for use in industrial environments and needs certain modifications to be used.

Harting developed the world's first industry-compatible attachable-in-the-field RJ45, and Hirose Electric miniaturised it.

Hirose is well-known for its expertise in miniaturizing high-performance connectors, including the micro-USB (USB2.0, 3.0 and 3.1) which the company originally developed. The result of the two companies joining forces is a new miniaturized and robust Ethernet interface for high-speed data transmission rates, aimed at establishing a new standard for Industry-4.0 applications.

"There is one thing that Industry 4.0 requires above all else: an Ethernet connection to each and every Industry 4.0 component," said Philip Harting, Chairman of the Harting Technology Board.

10-BIT HD OSCILLOSCOPES PROVIDE EXCEPTIONAL SIGNAL FIDELITY UP TO 4 GHz AND 40 GS/s

Teledyne LeCroy introduced the HDO9000 High Definition Oscilloscopes, which unveil HD1024 high definition technology that automatically optimizes vertical resolution under each measurement condition to deliver 10 bits of vertical resolution. The combination of the next-generation MAUI with OneTouch user interface with a big, bright, 15.4" touch screen takes oscilloscope efficiency, intuitiveness, and ease of use to a completely new level. The addition of the HD1024 technology to an exceptionally deep analysis toolbox enables the HDO9000 to easily uncover difficult to find signal abnormalities. The HDO9000 High Definition Oscilloscopes offer 10-bit resolution, bandwidths of 1 GHz to 4 GHz and sample rates of 40 GS/s, enabling efficient and accurate debug in high definition. Two units can be synchronized to operate as 8-Channel Oscilloscope without limitations, another unique feature in these high performance oscilloscopes.

HD1024 High Definition Technology

A critical element of the HDO9000 is the HD1024 technology, which provides 10 bits of vertical resolution with 4 GHz bandwidth. Waveforms are displayed clearly and crisply, unmasking fine signal details that cannot be seen on conventional 8-bit oscilloscopes. HD1024 technology enables the HDO9000 High Definition Oscilloscopes to automatically and dynamically determine the best ADC configuration under each specific measurement condition. Thus, the oscilloscope always provides optimal resolution. By utilizing optimized filtering the HDO9000 can provide additional resolution beyond 10 bits; extending up to 13.8 bits. As with all members of Teledyne LeCroy's HDO family, the HDO9000 sports an exceptionally low-noise system architecture that delivers outstanding effective number of bits (ENOB).

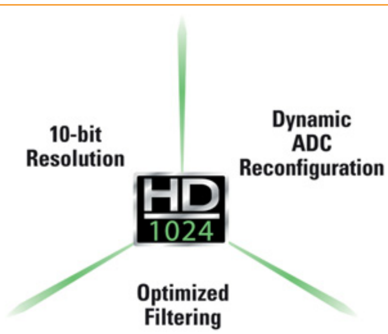

Figure 1: HD1024 technology enables 10 bits of vertical resolution with 4 GHz bandwidth

Debug in High Definition

In addition to the versatile standard toolset, Teledyne LeCroy offers a broad variety of optional software packages to equip the HDO9000 for all validation and debug requirements ranging from automated standards compliance packages to flexible debugging toolkits. A suite of protocol-specific measurement and eye diagram packages complements the industry's most intuitive trigger and decode software. The serial data packages augment HDO9000's already deep and powerful toolbox of math, measurement, debug, and documentation tools, bringing unsurpassed analysis capabilities to the bench or lab. Application-specific packages enable streamlined debug for common design and validation scenarios.

Superior User Experience with OneTouch

The HDO9000 with MAUI OneTouch sets the standard for oscilloscope user experience by providing the most unique touch features on any oscilloscope. Familiar touchscreen gestures are used to instinctively interact with the oscilloscope and dramatically reduce setup time. Convenience and efficiency are optimized - all common operations can be performed with one touch and do not require opening and closing of pop-up dialogs or menus.

MAUI with OneTouch introduces a new paradigm for oscilloscope user experience. Dramatically reduce setup time with revolutionary drag and drop actions to copy and set up channels, math functions, and measurement parameters without lifting a finger. Use common gestures like drag, drop, and flick to instinctively interact with the oscilloscope. Quickly enable a new channel, math or measurement using the "Add New" button and simply turn off any trace or parameter with a flick of the finger. These OneTouch innovations provide unsurpassed efficiency in oscilloscope operation.

Exceptional Serial Data Analysis

A wide variety of application packages is available to meet all serial data test challenges, ranging from automated compliance packages to flexible debug toolkits. A suite of protocol specific measurement and eye diagram packages is available to complement the industry's most intuitive trigger and decode packages.

Isolate events using the serial bus trigger and view color-coded protocol information on top of analog or digital waveforms. Timing

Figure 2: HDO9000 combines Serial Bus Trigger, Decode, Measure/Graph, and as industry first also the Eye Diagrams for the most advanced serial data analysis

and bus measurements allow quick and easy characterization of a serial data system. Measurement data can be graphed to monitor system performance over time. Identify physical layer anomalies with eye diagram mask testing and mask failure locator.

Unleash the power of serial data analysis to understand and characterize a design, proving compliance, and explain why a device or host fails compliance. The SDAII architecture provides fast updates and eye diagram creation. Combined with up to 128 Mpts record lengths and complete jitter decomposition tools, SDA II provides a fast and complete understanding of why serial data fails a compliance test. Whether debugging eye patterns or other compliance test failures, the HDO9000 Series rapidly isolates the source of the problem. Advanced jitter decomposition methodologies and tools provide more information about root cause. Tj Analysis, RjBUj Analysis and DDj Analysis are simplified with the deepest toolset dedicated to providing the highest level of insight into your serial data signals.

Very Powerful, Deep Toolbox

The standard collection of math, measurement, debug, and documentation tools provides unsurpassed analysis capabilities. Application-specific packages enable streamlined debugging for common design/validation scenarios. The advanced customization option enables user-defined parameters and math functions providing unique and limitless analysis capability.

Teledyne LeCroy's 50+ year heritage has its origins in the high-speed collection of data in the field of high-energy physics, and the processing of long records to extract meaningful information. We didn't invent the oscilloscope, but we did invent the digital oscilloscope, which can take full advantage of advanced digital signal processing and waveshape analysis tools to provide unparalleled insight.

Our developers are true to our heritage – they are more obsessed with making better and smarter tools than anybody else. Our mission is to help you use these tools to understand problems, including the ones you don't even know you had. Our deep toolbox inspires insight; and your moment of insight is our reward. Teledyne LeCroy provides more powerful, more unique, and more standard tools than any other oscilloscope company, and much of what is now "standard" in competitive products originated at Teledyne LeCroy. Our tools and operating philosophy are standardized across much of our product line for a consistent user experience from 200 MHz to 100 GHz. Our MAUI advanced user interface makes the tools easy to access, use, and combine in powerful ways to solve unique problems.

Our Periodic Table of Oscilloscope Tools provides a framework to understand the toolsets that Teledyne

LeCroy has created and deployed in our oscilloscopes. Visit our interactive website to learn more about what we offer and how we can help you develop and debug more efficiently.

Powerful Mixed-Signal Capabilities

With embedded systems growing more complex, powerful mixed signal debug capabilities are an essential part of modern oscilloscopes. The 16 integrated digital channels and set of tools designed to view, measure and analyze analog and digital signals enable fast debugging of mixed-signal designs.

Using the powerful parallel pattern search capability of WaveScan, patterns across many digital lines can be isolated and analyzed. Identified patterns are presented in a table with time-stamped information, speeding up the search for each pattern occurrence. Use a variety of the many timing parameters to measure and analyze the characteristics of digital buses. Powerful tools like tracks, trends, statistics and histicons provide additional insight and help to detect anomalies. Check the state of all the digital lines simultaneously using convenient activity indicators. Simulate complete digital designs using logic gate emulation. When used with the web editor, many logic gates can be combined in one math function to simulate complex logic designs. Choose from AND, OR, NAND, NOR, XOR, NOT and D Flip Flop gates.

For applications demanding even higher-performance mixed-signal acquisition capabilities, the HDA125

High-speed Digital Analyzer can be easily added to the HDO9000. With 12.5 GS/s digital sampling rate on 18 input channels and the revolutionary QuickLink probing solution, validation of challenging interfaces such as DDR memory has never been simpler or more comprehensive.

teledynelecroy.com

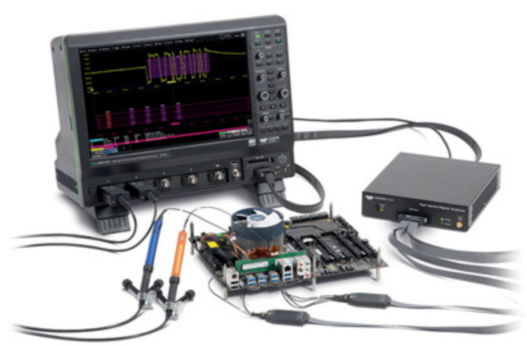

Figure 3: With 12.5 GS/s digital sampling rate on 18 input channels and the revolutionary QuickLink probing solution, validation of challenging interfaces such as DDR memory has never been simpler or more comprehensive

Exploring the IoT Sensor Badge

BY **LUCIO DI JASIO**, MCU8 BUSINESS DEVELOPMENT MANAGER AT MICROCHIP TECHNOLOGY

I recently started using IoT Sensor Badge, a sleek little promo board featuring the latest generation PIC microcontrollers (PIC16F18345), five NeoPixel LEDs, an accelerometer and a temperature sensor.

I might have been attracted to it because of its fancy name, or it could have been its colorful blinking lights – it's difficult to tell, but I ended up a happy owner of one of them.

I won't get into the semantics of the Internet of Things (IoT), but in my current understanding there are some minimum features of the IoT Sensor Badge board:

- **Communication, preferably wireless.** There is a Bluetooth Low Energy (BLE) (RN4020) module on the back of the board.
- **Low power consumption.** The entire board is powered by a single 1.5V alkaline battery. A tiny booster circuit (MCP16252) manages to bring the voltage to 3V to power the BLE module and LEDs.
- **Environmental awareness.** Various on-board sensors are used for distinguishable colour and sound patterns.

The combination of these features may suggest novel application ideas, perhaps something wearable, but I have already come up with some ideas to show my (pre-teen) son the magic of wireless connectivity. At that point however, I realized what was truly missing from my project is a proper iOS app.

As usual, for me a shortcoming is also a challenge. (My passion for learning new programming languages made me learn Swift, the new official Apple apps development language. I also recently learned about Pythonista 3, an iOS app that promises to make developing iOS applications a breeze using the Python language.) So, what I needed was an understanding of the protocol used by the IoT Badge to communicate. Critically, despite the complete set of source files, BOM, schematics and other collaterals available for download, the actual communication protocol's documentation was nowhere to be found on the product page. This led to a short investigation:

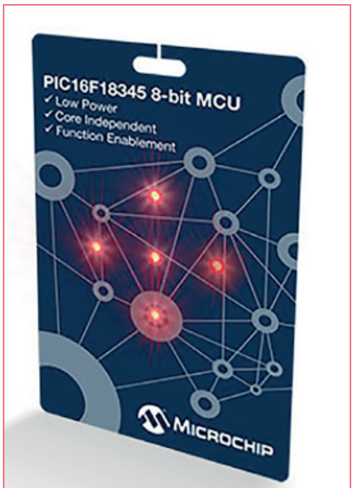

Figure 1: The IoT Sensor Badge

Figure 2: Pythonista 3

1. MPLAB X Project Forensics

On the IoT Badge promo page is a link to a downloadable MPLAB X project (zip) file, which contains a source file called "RN4020.c" – a clear reference to the little BLE module. Sadly this only contained some initialization code, but it did reveal one precious detail: the BLE module was going to be used in MLDP mode (more on this later).

I then looked inside the "interrupt.c" file, where I expected only interrupt service routines. Hidden within the serial port (EUSART) ISR was a section of code that handled each character received (from the BLE module) and compared it against a set of only three possible ASCII values:

```
if (RCREG == '%') { //BUTTON1 PRRESS
PIRobits.IOCIF = 1;
IOCBFbits.IOCBF5 = 1;
}
```

```
if (RCREG == '#') { //BUTTON2 PRRESS
PIRobits.IOCIF = 1;
IOCBFbits.IOCBF7 = 1;
}

if (RCREG == '$') { //Send requested data
Temp9700Read();
CalcVBattery(); //Get batter voltage
TRISCbits.TRISC4 = 0; //NCO on
NCO1INCL = 10;

sprintf(s, "@%d, %d, %d, %d, %d, %d, %d, %d, %d, %d, %d,
%d, %d, %d, %d, ", G1, R1, B1, G2, R2, B2, G3, R3, B3, G4,
R4, B4, G5, R5, B5); //LED data
USARTWriteString(s);
sprintf(s, "%d, %d, %d, %d\r\n", (int8_t) Roll, (int8_t)
Pitch, (int8_t) TEMP_F, BATTV); //XYZ, TEMP & BAT
USARTWriteString(s);
```

Listing 1: Interrupt.c – a snippet

When '%' or '#' characters are received, a corresponding button-press event is "simulated" by triggering manually the Interrupt On (pin) Change mechanism. This is a technique I would not generally recommend but, at least in this case, appears effective.

When a '$' character is received instead, the device immediately launches a sequence of calls to update its temperature and battery voltage readings. Again, I wouldn't recommend such lengthy operations in an interrupt context, but the simplicity of the application seem to be forgiving of the somewhat sloppy design practice.

Eventually a long string appears to be sent back to the BLE module containing the following:

- The '@' character;
- 5x NeoPixel colour coordinates as green, red, blue triplets;
- The last (cached) value of the roll and pitch angles (in degrees) computed from the accelerometer's last reading;
- The temperature, in degrees Fahrenheit;
- The battery voltage, in Volts.

A pair of Carriage Return and New Line ('/r', '/n') end the string.

Note how all values are sent in decimal notation and are comma and space separated! This makes for a long but readable format, although not exactly an easily parsed one.

2. MLDP Revealed

MLDP is a solution Microchip offers to embedded developers looking for a quick way to emulate a serial point-to-point connection over BLE.

In the original Bluetooth (3.x) standard, the Serial Profile (SPP) provided this as a standard option, out of the box. With BLE (4.1), the old profiles have been replaced by GATT, a very flexible (and power-efficient) way to define and handle data transfer via the sharing and remote update of "characteristics".

MLDP brings back the simplicity of a serial profile to BLE systems by offering an alternate mode of communication between the BLE module (RN4020 for example) and the host microcontroller serial port. Once the BLE module enters MLDP mode (by means of an I/O selection or a special command sequence), all other details of the BLE protocol are abstracted away and, as soon as a connection with a paired device is established, the two connect through a full bidirectional serial communication link.

The official Microchip documentation is careful to avoid the low-level implementation details – how MLDP translates into GATT services and characteristics – perhaps to preserve the fullest abstraction.

Fortunately, by using Microchip's own tools, such as Bluetooth Smart Data or Smart Discover (both available in the Apple Store), it is quite easy to figure out the key identifiers (UUIDs) of the MLDP service and its Data characteristic:

MLDP_SERVICE = '00035B03-58E6-07DD-021A-08123A000300'

MLDP_DATA = '00035B03-58E6-07DD-021A-08123A000301'

Armed with this information, I was now ready to move on to the iPad (or iPhone) and create a short Python script.

3. Implementing MLDP In Python

Pythonista 3 Core Bluetooth module (a built-in library) wraps nicely the functionality of the iOS BLE framework and can easily be adapted to fit the IoT Badge Sensor application. All logic can be encapsulated in a single "class" whose methods will be used

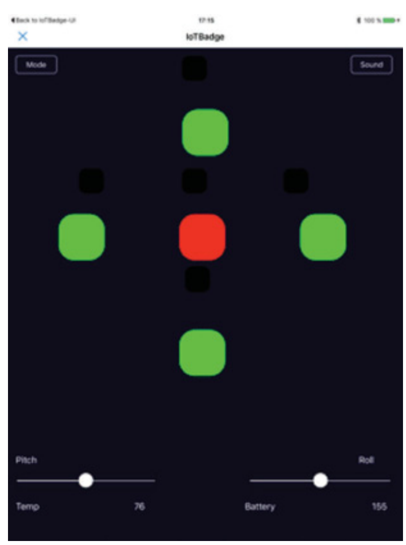

Figure 3: IoT Sensor Badge iPad UI

as delegate functions (this is computer science lingo for "callback functions" in embedded control) for each step of the BLE connection process.

```
class MLDPManager (object):
def __init__(self):
self.peripheral = None
self.buffer = "

def did_discover_peripheral(self, p):
def did_discover_services(self, p, error):
def did_discover_characteristics(self, s, error):
```

Listing 2: cb manager class template

For example, once a service is "discovered" we can compare its identifier (UUID) with that of the MLDP_SERVICE found above, and immediately launch a search for the corresponding DATA characteristic:

```
def did_discover_services(self, p, error):
for s in p.services:
if s.uuid == MLDP_SERVICE:
p.discover_characteristics(s)
```

Listing 3: MLDP_manager, did_discover_service callback

Similarly, once the DATA characteristic is found, we can enable the 'notification' feature and store the resulting 'handle' (data_char) for later use during the communication data transfer phases:

```
def did_discover_characteristics(self, s, error):
for c in s.characteristics:
if '301' in c.uuid:
self.data_char = c
# Enable notification for MLDP input:
self.peripheral.set_notify_value(c, True)
```

Listing 4: MLDP_manager, did_discover_characteristic callback

Sending data or a command through the MLDP connection to the IoT Sensor Badge is now possible, simply by assigning a new value to the DATA characteristic:

```
def send_cmd(self, cmd):
if self.peripheral:
self.peripheral.write_characteristic_value(self.
data_char, cmd, True)
```

Listing 5: MLDP_manager, send_cmd method

When the IoT Sensor Badge starts sending new data, there will be a notification. That is, *did_update_value* delegate (callback) will be invoked:

```
def did_update_value(self, c, error):
self.buffer += c.value.decode('ascii')
if self.buffer[-1] in '\n':
if self.buffer and self.buffer[0] == '@':
print(self.buffer[1:]) # send to console
self.buffer = "
self.send_cmd(b'$') # ask immediately for more...
```

Listing 6: MLDP_manager, did_update_value callback

Since the BLE protocol allows each characteristic to pass a maximum of 20 characters (bytes) at a time, the *did_update_value* delegate must perform a bit of buffering to re-assemble the longer strings the IoT Sensor is likely to send.

4. In 10 Lines Of (Python) Code

Pythonista 3 introduces a simple console view for iOS applications to provide a quick way to present data (and receive inputs) from the user without necessarily requiring a complete GUI to be defined.

A few more lines of code give us a quick way to test the code developed this far:

```
mngr = MLDPManager()
cb.set_central_delegate(mngr)
cb.scan_for_peripherals()
while not mngr.peripheral:
pass
mngr.send_cmd(b'$')
```

Listing 7: Application main

This code launches the Bluetooth core manager, waits for the connection to be established with the first IoT Sensor Badge found, then triggers an update process by sending the first '$' command. The process will continue indefinitely as the last line of each *did_update_value* callback triggers a new request for data (see Listing 6). This will quickly fill the iPad/iPhone screen with strings sent by the IoT Sensor. Soon you will want to stop the script (using the little button at the top right of the Pythonista 3 console) and inspect the data.

If you are like me, this will be only the beginning of the exploration. You will soon itch to create a bit of UI for the application, perhaps mimicking the IoT Badge faceplate (see Figure 3). The complete code for this project has been posted on Github (**https://github.com/luciodj/IoTBadge-UI**).

Unfortunately, a complete description is beyond the scope of this short article, but (spoiler alert) will turn out to be a very quick and pleasant experience as the Pythonista 3 (GUI) library wraps elegantly around the iOS native UI frameworks. ●

Using ultraviolet sensors in embedded designs

BY **DR DOGAN IBRAHIM**, PROFESSOR AT THE NEAR EAST UNIVERSITY, CYPRUS

Sun-generated ultraviolet (UV) radiation reaches the Earth, with all its positive and negative effects. UV is invisible to the naked eye as its wavelengths are shorter than visible light; it is classified as UVA, UVB and UVC – see Figure 1.

Some 95% of the Sun's rays reaching planet Earth are UVA, of 320-400nm wavelength, able to penetrate clouds and glass, but also absorbed by the ozone layer. UVA is known to cause skin tanning but also ageing, wrinkling and skin cancer, since it penetrates the skin deeper than UVB, doing more damage.

UVB rays have shorter wavelengths of 280-320nm, helping the body generate Vitamin D. Most UVB rays are absorbed by the atmosphere before they reach the Earth's surface, but some 0.1% get through. Known as "burning rays", they have been associated with 65% of skin tumours.

UVB rays do not penetrate glass.

UVC type radiation have even shorter wavelengths, 100-280nm. Although they can be harmful, all are absorbed by the ozone layer and do not reach the Earth's surface.

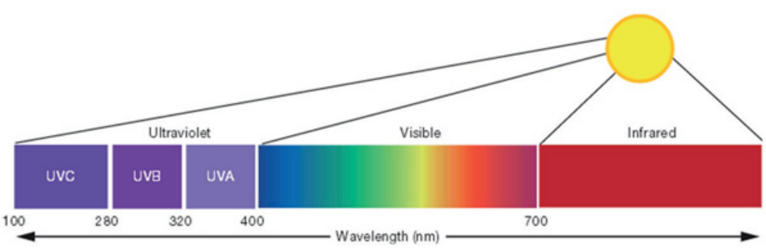

Figure 1: Wavelengths of the UV radiation

UV Index	Risk from unprotected exposure	Protection
0 – 2	LOW	Low risk. Wear sunglasses on bright days
3 – 5	MODERATE	Moderate risk. Apply SPF 30+ sunscreen
6 – 7	HIGH	High risk. Reduce time in the sun. Apply SPF 30+ sunscreen every 2 hours
8 – 10	VERY HIGH	Very high risk. Minimize sun exposure between 10am-4pm. Apply SPF30+ sunscreen
11 -	EXTREME	Extreme risk. Avoid sun exposure between 10am-4pm. Apply SPF30+ sunscreen

Table 1: UV index table with recommended protection

UV Light Effects

The effects of UV rays depend on many factors, including:

- Time of day: UV rays are strongest between 10am and 4pm;
- Season: UV rays are stronger in the summer months;
- Distance from the Equator: UV rays increase in intensity closer to the Equator;
- Cloud cover: some clouds absorb some UV radiation;
- Reflection from surfaces: UV rays can reflect from surfaces like water, snow, or grass, leading to increased exposure.

Because of the complexities of these factors, a UV index has been developed to indicate how strong the UV light is in a given area. The index is on a scale from 1 to 11+, where a higher number means stronger UV light and therefore greater risk of exposure and higher chance of skin damage, sunburn or skin cancer.

Table 1 shows the UV index with recommended protection. The efficacy of sunscreen protection creams is measured in SPF (sun protection factor), which indicates how long it will take for UVB rays to redden the skin with the cream compared to without it. For example, SPF 30 will take 30 times longer to redden without sunscreen. SPF 15 sunscreen protects 93% of the UVB rays; SPF 30 protects 97% and SPF 50 protects 98%. It's important to select a sunscreen that protects against both UVA and UVB rays.

The UV indexes are normally published by the meteorological stations in every country for different times of day and different days of a month. As an example, Figure 2 shows the UV index for the UK on a cloudy summer's day.

The UV index is related to irradiance (measured in W/m^2) and its calculation is a complex process, depending on the measured UVA and UVB radiation at the place of interest. Figure 3 shows the strength of irradiance versus the UV index.

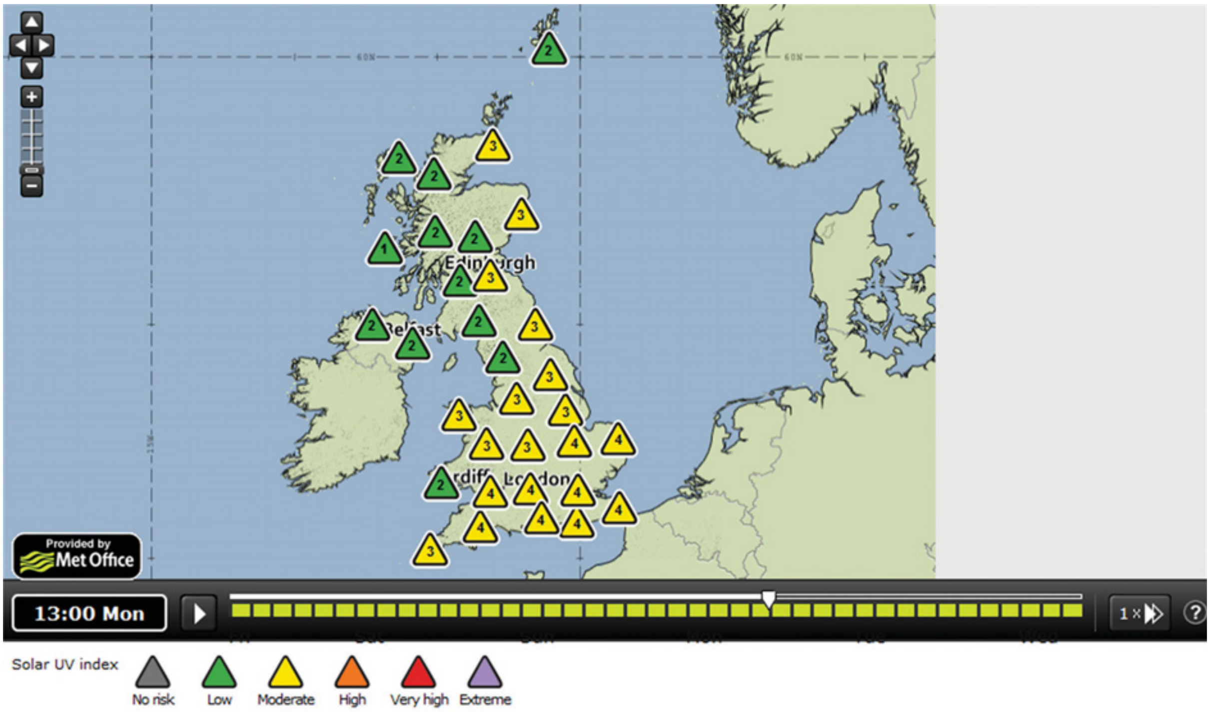

Figure 2: The UV index on a particular day in the UK (source: www.metoffice.gov.uk)

UV Sensors

UV sensors are light sensors at heart, designed to be sensitive to wavelengths in the UV range of the spectrum. In most UV sensors UVA and UVB are combined in a single package. UV safety sensors may also include a UVC sensor in the same package, if needed.

The working principle of UV sensors is very simple: Photons hit a certain semiconductor material, which reacts by emitting electrons or by changing its electrical characteristics. The changes in current are then processed to determine the type and amount of radiation.

Some commonly used UV sensors are shown here. The ML8511 (Figure 4) from SparkFun is a small analogue output UVA/UVB sensor in the range 280-390nm. Its output voltage is 1-3V, and is linearly dependent on the UV intensity up to 15mW/cm².

GUVA-S12SD is an UVA/UVB sensor module from Adafruit (Figure 5) in the range 240-370nm. The analogue signal output from its photodiode is very small, so an op-amp is used to amplify the signal to manageable levels.

Skye Instruments UV sensors (Figure 6) measure UVA and UVB radiation, providing analogue output signals proportional to the measured irradiance.

Example UV Index Meter

This section presents a microcontroller-based UV meter with LCD output; see Figures 7 and 8.

UV2 Click is a microbus-compatible UVA/UVB sensor module

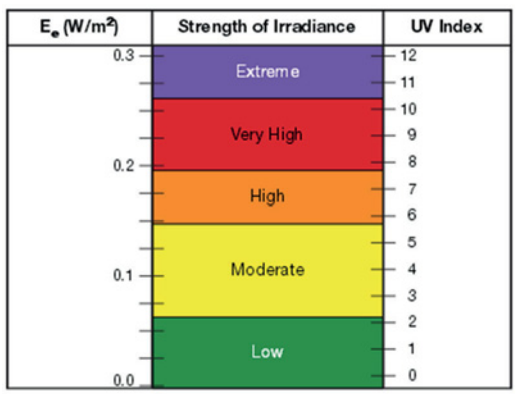

Figure 3: Strength of irradiance and the UV index

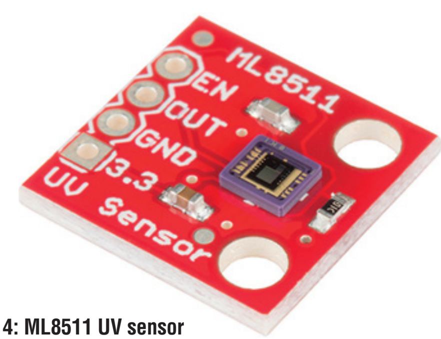

Figure 4: ML8511 UV sensor

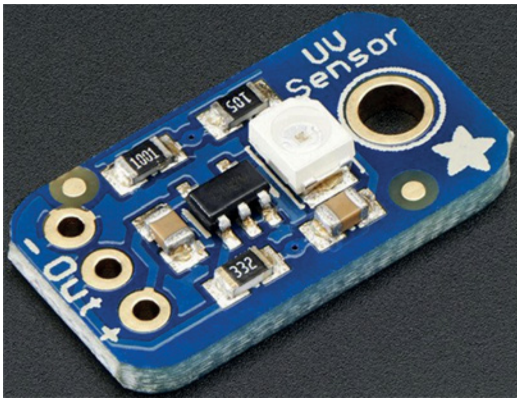

Figure 5: GUVA-S12SD UV sensor

Figure 6: Skye Instruments UVA sensor

that uses the VEML6075 light sensor chip. UV light intensity is converted into a 16-bit digital value with the UVA and UVB values read from different channels. The chip is temperature-compensated to ensure correct operation in long hours of exposure to sunlight.

UV2 Click (see Figure 8) operates from 3.3V and uses the I2C bus for communication. Current consumption is around 480μA. The module is most sensitive to UVA at 350-375nm and UVB at 320-340nm. The two I2C control lines SCL and SDA connect to the mikroBUS edge connector through two 4.7K on-board pull-up resistors, as required by the I2C protocol.

EasyPIC V7 is a microcontroller development board that uses the PIC18F45K22-type medium-performance PIC microcontroller, operating at 8MHz. This board contains sockets for GLCD, LCD, 4-digit 7-segment display, RS232 interface, 36 LEDs and 36 push-button switches, USB-UART interface and more. It has two mikroBUS sockets; the UV2 Click module is connected to socket 1. A 16x2-character text-based LCD displays the calculated UV index.

The system circuit diagram is shown in Figure 9. UV2 Click SCL and SDA lines are connected to the PIC microcontroller I2C control lines RC3 and RC4 respectively; the LCD is connected to PORTB in 4-bit data mode.

The Software

This project's software was developed using the mikroC Pro for PIC language and IDE. The developed program was loaded to the target microcontroller using the on-board mikroICD debugger/programmer. The complete program is shown in Listing 1.

The interface between the LCD and the microcontroller is defined at the beginning of the program. Once the LCD, the I2C bus and sensor chip are initialized, the program also configures PORTB and PORTC as digital outputs.

The address of the sensor chip is 0x20. The remainder of the program is executed in an endless loop, inside which function Get_UV is called to read the current UVA and UVB values from the sensor. Then, function Get_UV_Index is called to calculate the UV index.

The UV index is a floating point number which is converted into a string to be displayed on the LCD every second.

The UV index is calculated using the following equations (see the VEML6075 sensor data sheet for more information):

$$\mathbf{UVA_{comp} = (UVA - UVD) - a*(UV_{comp1} - UVD) - b*(UV_{comp2} - UVD)}$$
$$\mathbf{UVB_{comp} = (UVB - UVD) - c*(UV_{comp1} - UVD) - d*(UV_{comp2} - UVD)}$$

where UV_{comp1} and UV_{comp2} are noise-compensation channels and UVD is a dummy channel that allows the other UV channels to cancel out the dark current or any stray light injection to the silicon substrate.

Constants a, b, c, and d have the following values in open-air systems without a diffuser:

a = 3.33
b = 2.5
c = 3.66
d = 2.75

The UV index (UVI) is then given by:

$$\mathbf{UVI = [(UVB_{comp} * UVB_{res}) + (UVA_{comp} * UVA_{res})]/2}$$

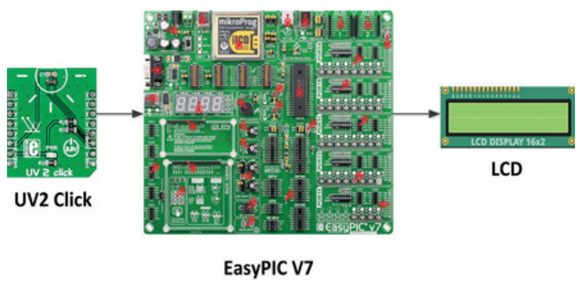

Figure 7: Microcontroller-based UV meter with LCD output

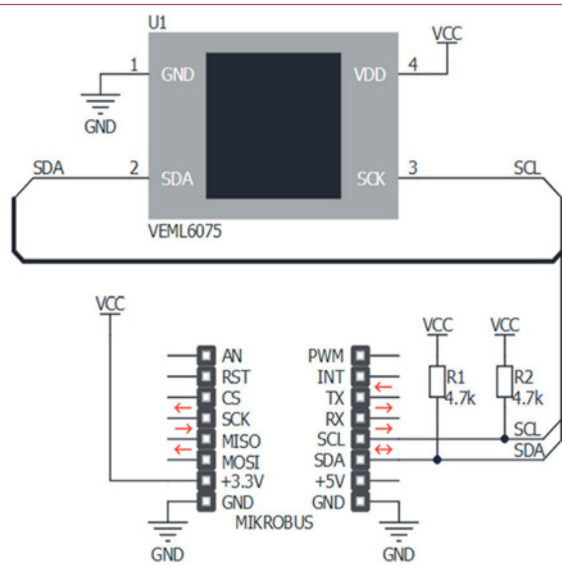

Figure 8: The UV2 Click module pinout diagram

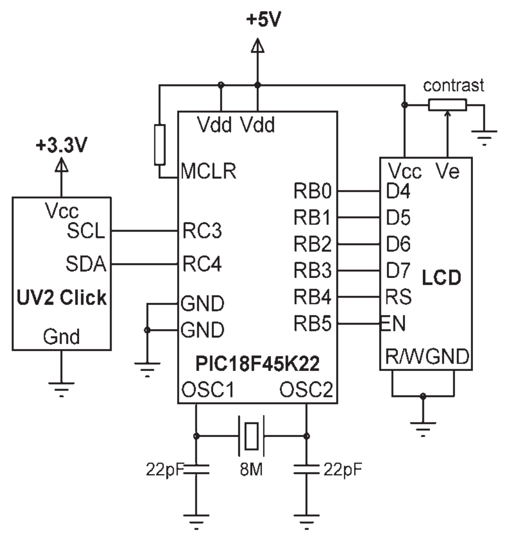

Figure 9: UV meter connections

where UVA_{res} and UVB_{res} are the UVA and UVB responsivity parameters, with values of 0.0011 and 0.00125 respectively.

Floating-point calculations are used throughout the program. Although it is possible to display the UVA and UVB readings as well, for simplicity in this project only the UV index is displayed. ●

```
sbit LCD_RS at RB4_bit;
sbit LCD_EN at RB5_bit;
sbit LCD_D4 at RB0_bit;
sbit LCD_D5 at RB1_bit;
sbit LCD_D6 at RB2_bit;
sbit LCD_D7 at RB3_bit;

sbit LCD_RS_Direction at TRISB4_bit;
sbit LCD_EN_Direction at TRISB5_bit;
sbit LCD_D4_Direction at TRISB0_bit;
sbit LCD_D5_Direction at TRISB1_bit;
sbit LCD_D6_Direction at TRISB2_bit;
sbit LCD_D7_Direction at TRISB3_bit;
float UVA,UVB,UVcomp1,UVcomp2,UVD,UVAcomp,
UVBcomp,UVI;

unsigned int Get_UV(unsigned char reg)
{
 unsigned char temp[2];
 unsigned int retval;
 I2C1_Start();
 I2C1_Wr(0x20);
 I2C1_Wr(reg);
 I2C1_Repeated_Start();
 I2C1_Wr(0x21);
 temp[0] = I2C1_Rd(0);temp[1] = I2C1_Rd(0);
 retval = (unsigned int)temp[0];
 retval |= ((unsigned int)temp[1]) << 8;
 I2C1_Stop();
 return retval;
}

void Get_UV_Index()
{
 float a = 3.33, b = 2.5, c = 3.66, d = 2.75;
 float UVAres = 0.0011, UVBres = 0.00125;
 UVAcomp=(UVA-UVD)-a*(UVcomp1-UVD)-
b*(UVcomp2-UVD);
 UVBcomp=(UVB-UVD)-c*(UVcomp1-UVD)-
d*(UVcomp2-UVD);
 UVI=((UVBcomp*UVBres)+(UVAcomp*UVAres))/2;
}

void Init_Sensor()
{
 I2C1_Start();
 I2C1_Wr(0x20);
 I2C1_Wr(0x00);
 I2C1_Wr(0x00);
 I2C1_Wr(0x00);
 I2C1_Stop();
}

void main()
{
 unsigned char Text[14];
 ANSELB = 0;
 ANSELC = 0;
 LCD_Init();
 I2C1_Init(100000);
 Init_Sensor();

 while(1)
 {
 UVA = (float)Get_UV(0x07);
 UVD = (float)Get_UV(0x08);
 UVB = (float)Get_UV(0x09);
 UVcomp1 = (float)Get_UV(0x0A);
 UVcomp2 = (float)Get_UV(0x0B);
 Get_UV_Index();
 FloatToStr(UVI,Text);
 LCD_Cmd(_Lcd_Clear);
 Ltrim(Text);
 Lcd_Out(1,1,Text);
 Delay_Ms(1000);
 }
}
```

Listing 1: The UV meter program

Modern SoCs' Thermal Issues

BY **OLIVER KING**, CHIEF TECHNOLOGY OFFICER OF MOORTEC

Gate density has been increasing with each node, pushing up power per unit area in semiconductors. This issue is even greater in FinFET processes, where channels are more thermally isolated than in planar structures.

Then there is leakage, which in the last few planar nodes led to significant power consumption. That has been pegged back somewhat with the latest FinFET nodes but power consumption will continue to be a problem going forward.

In addition, in developing consumer products, and especially portable devices, there will always be power limitations; in such devices there are no active cooling systems such as fans, so the upper temperature limit must be quite low. Then, the hotter the device gets, the bigger the problems with reliability and operational lifetime of parts – which I'd say is perhaps the biggest issue going forward, as we are then entering the realm of electro-migration, hot carriers and bias temperature instability (BTI).

Degrees Of 'Hot'?

"How hot is hot?" depends on the application! That said, there are some applications where we are starting to see higher temperatures – in automotive for example, with ADAS and infotainment applications, where even 125°C is not high enough as they demand higher and higher temperature operation.

So there are different temperature ranges, depending on the end market: in automotive this may be higher than 125°C, yet in consumer 40°C might be the limit. And if thermal mass is factored in, there will be much hotter devices within a product range.

Nevertheless, the key thing is to accurately know the device's temperature, so it can operate closer to the limit. And this is the crux with modern SoCs: being as close as possible to the limit without overstepping it.

Use Trends

Temperature has an exponential effect on device ageing, so the accuracy of temperature sensors is correspondingly important.

Several years ago, when we started developing temperature sensors, they were used largely for device characterisation, high-temperature operating life (HTOL), burn-in tests and so on. Back then they, they were used for high temperature alarms, either to switch off a device or turn on a fan. But over the last couple of years we've begun to see more applications that rely on these monitors; applications like dynamic voltage and frequency scaling (DVFS), adaptive voltage scaling (AVS) and lifetime reliability. Recent trends have been driven by consumer electronics, where a lot is demanded from a device without it getting too hot, since it may operate in someone's pocket, hands or lap.

We are already into the realm where the costs of advanced node technologies drive a trend to 'extract' everything out of a device, with many different levels of overdesign added to the processes and the design flow which may inevitably take away from the device's performance. As a result, on-chip sensors, whether for temperature, process or voltage sensors, will allow getting that little more performance and/or improving reliability without slowing down the device.

Temperature Sensors Demands

So we can see that accurate device temperature plays a crucial role in its design: the greater the uncertainty in the measured result, the less it can be asked to do. Beyond that, the next most important issues are robustness and testability, because these sensors are now in applications where their failure can cause complete system failure; so they need to be able to be tested whilst in operation, for complete reliability.

There are sensors that enable online fault detection and diagnosis; they can be interrogated to determine where a fault is and learn its diagnosis. Scan chains can be supported to increase overall test coverage.

On top of all this, we believe ease of integration is an important factor – not because it yields a more accurate temperature sensor, but because it makes it easier for the customer to implement and use the product. ●

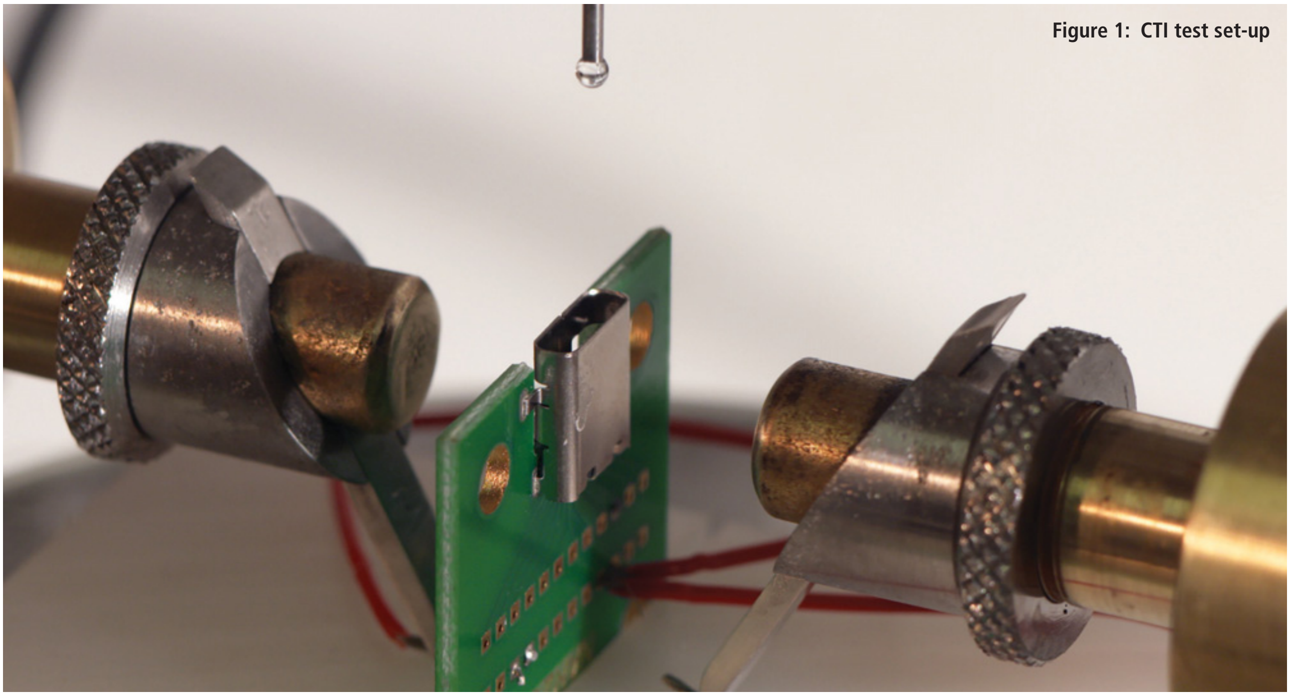

Figure 1: CTI test set-up

HIGH-PERFORMANCE BIOPLASTICS ENABLE "GREEN" ELECTRONIC DESIGNS

KONRAAD DULLAERT, GLOBAL BUSINESS MANAGER FOR FORTII, AND **JOHN HSIEH**, INDUSTRY SEGMENT LEAD FOR CONNECTORS, BOTH AT DSM, LOOK AT PLASTICS AND POLYMERS FOR ELECTRONIC COMPONENTS NOW AND GOING FORWARD

The drive continues in the electronics industry to integrate more functionality into even smaller spaces. This obviously has important implications for designers and producers of components such as device housings and connectors, which need ultrathin walls yet still work perfectly – mechanically and electrically. At the same time, plastics at the heart of electronic devices should withstand manufacturing and assembly rigours. This means, above all else, they must resist the high temperatures of soldering.

On top of that, especially for consumer electronics, there is need for materials that are not hazardous for health and the environment. This boils down to two things: plastic components made with halogenated additives – principally flame retardants, but also pigments – are rapidly falling out of favour; plastics produced, at least in part, from renewable resources are especially welcome!

> "Audio jacks located along the sides of mobile phones are the limiting factor on how thin the phones can be made

Furthermore, electronics companies with a focus on US governmental business are being requested to obtain EPEAT (Electronic Product Environmental Assessment Tool) certification; all of the criteria used in EPEAT are based on ANSI-approved public standards within IEEE 1680.

Whilst in general a basic EPEAT Bronze certification is enough, companies have started to target silver or even gold ratings to differentiate themselves from the competition. A gold level is not achievable without a close strategic look into the plastics used in product design, and giving strong consideration to the use of recycled and bio-based plastics.

High Temperature Polyamides

One of the most commonly used polymer families for high-performance components such as connectors is polyphthalamides, or PPAs. These are chemically related to the more common polyamides (nylons), but their structure gives them better resistance to high temperatures. PPAs come in various guises with varying properties, both in terms of processability and end-use suitability.

PPAs compete with liquid crystal plastics (LCPs) in connectors that need to resist the high temperatures found in reflow soldering of surface-mount technology (SMT) components. LCPs have a large share of the market, owing to their very good processability, low warpage and inherent flame retardance. Shortly into the 21st century, PPAs began replacing LCPs because they provided better mechanical properties and colourability.

The ongoing need for further miniaturization, such as overall dimensions and the distance between connector pins or strips (pitch), created quite a strong push for PA4T-based compounds: these provide a unique balance of very high temperature resistance, superior mechanical strength and high melt-flowing capabilities, making them suitable for I/O connectors such as audio jacks in mobile electronics and the new USB Type-C connector system, terminal blocks, power connectors and DDR DIMM connectors.

USB-C

The USB Type-C connector is a major challenge for companies supplying plastics for insulating components, both in terms of design and manufacturing. That is because it is much smaller than its predecessors and, yet, has to handle much more power.

The many connecting strips on the USB Type-C connector are spaced with a pitch of just 0.5mm, compared with 0.65mm on a USB 3.0 Micro B and 2.0mm on a USB Type A connector.

The thinnest insulating wall has come down from 1.84mm on the USB Type A to a much thinner 0.12mm on the USB Type-C connector. It is extremely difficult to successfully design and consistently mould parts with such thin walls that have the necessary mechanical and – critically – electrical properties.

Many component producers began developing the new USB Type-C connector using LCPs. These polymers are well-known by USB connector makers, since they are the favoured polymer in previous generations of USB. But, in many cases, USB Type-C connectors moulded in LCPs are likely to fail stringent electrical tests, especially resistance to surface tracking, expressed as Comparative Tracking Index (CTI).

The CTI of a plastic that acts as an insulator in an electronic component is more than ever crucial for product reliability. If the insulator does not have sufficiently high CTI, there is a high risk that at some point during use a short circuit will result from environmental (conductive) particle contamination triggered by, for example, sweat, moisture or dust, damaging the entire device and possibly even starting a fire.

In recent years, there have been several reports of mobile devices catching fire during charging or being damaged due to surcharges. Some halogen-free polyamides, including 46 and 4T, qualify for the highest material rating, group I, which indicates a CTI in the 600V range; LCPs on the other hand fall into the lowest material rating group, IIIa, with a CTI between 100V and 175V.

In tests where the ingress of sweat or moisture was simulated on USB Type-C connectors of identical design but with different insulating polymers (LCP and PA46), the connectors with the LCP showed significantly less resistance to surface tracking, with the insulator actually becoming carbonized; PA46 and PA4T-based USB Type-C connectors show more than twice the electrical robustness, as can be expected from their high CTIs. In addition, the halogen-free flame retardant additive systems they incorporate provide a UL 94 rating as high as V-0 at 0.2mm.

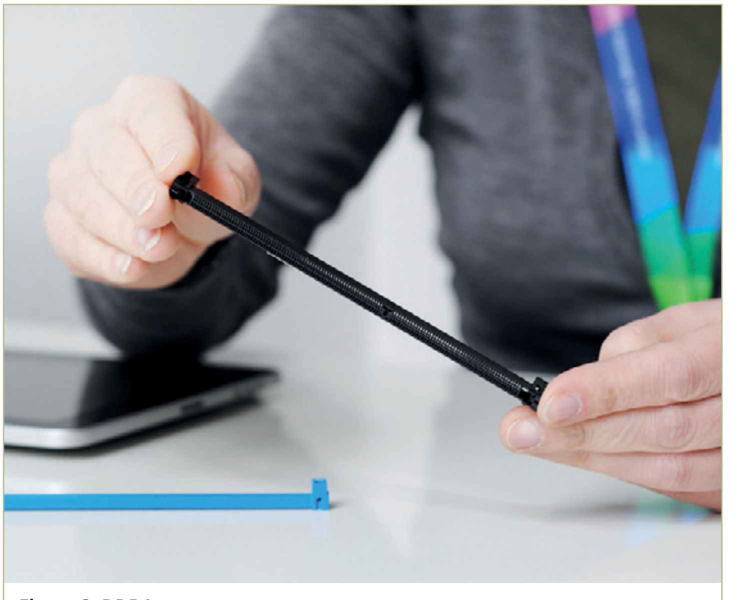

Figure 2: DDR4 memory connector

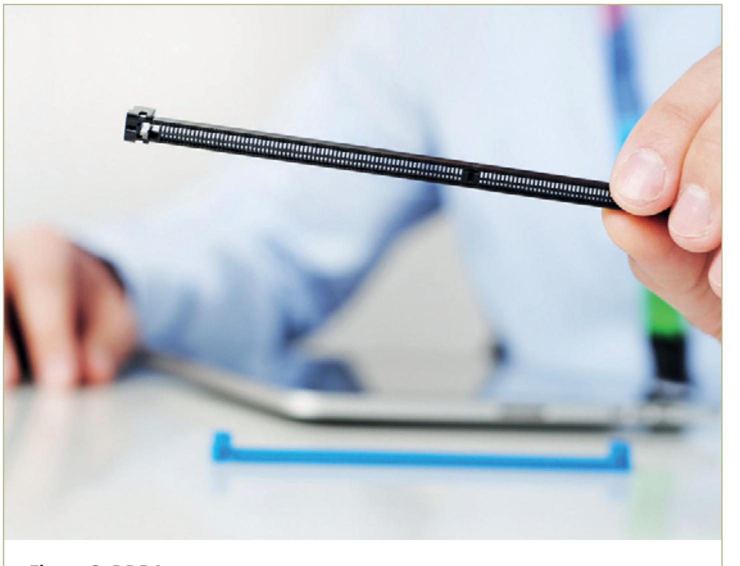

Figure 3: DDR4 memory connector

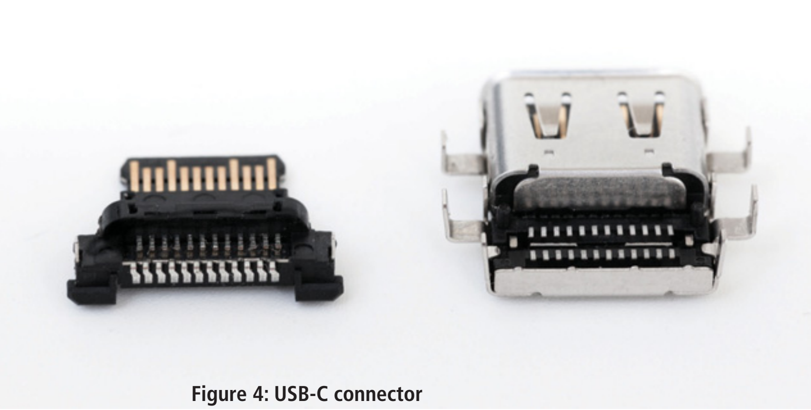

Figure 4: USB-C connector

Figure 5: USB-C connector

DDR4 And DDR5 Connectors

Polyamides like 46 and 4T provide a reliable and safe solution, offering the best balance of mechanical and electrical properties and precision moulding capability. They also have very good wear resistance: parts successfully pass durability tests that involve mating and unmating plugs and sockets over 10,000 times. They have already been approved by several global producers for use in USB Type-C connectors and are being used in millions of USB Type-C connectors on the market, on the plug as well as the receptacle side.

Further important advantages for high-performance polyamides such as 46 and 4T in this application include their compatibility with ultrasonic welding used in some designs for joining separate connector components together.

Polyamide 4T is also specified by several producers of DDR4 connectors widely used in servers, who appreciate the material's good flow, mechanical properties and its ability to produce connectors with low side-wall collapse and low warpage. DDR4 connectors are around 16cm long and contain 288 separate contacts. Very few thermoplastics can be made into such parts while resistant to the soldering temperatures (up to 280°C) used in SMT. The choice is even smaller when DDR5 becomes a reality; however, early testing of DSM's Stanyl PA46 and ForTii PA4T according to the new DDR5 specification, shows that both materials meet DDR5's further increased requirements in terms of flow, warpage, side wall collapse and dielectrics.

DDR5 prototype systems were shown during the IDF (Intel Developer Forum) in early 2016 by companies such as Rambus, where Stanyl-based connectors easily passed all tests according to the full DDR5 specification (an important difference between DDR4 and DDR5 connectors is that the latter operate at frequencies of 6.4GHz, twice that of DDR4).

Combining Assembly Techniques

A more recent PCB assembly technique is Pin In Paste, or PIP, used to increase productivity in device production by simplifying the soldering processes. In the past, many boards had components that required a combination of reflow and wave soldering, where SMT components were soldered first, followed by a second wave soldering process for PTH (Pin Through Hole) components. Because PTH uses lower temperatures, PTH parts can be moulded using plastics with lower thermal stability, including PA66 and PBT.

But, this two-stage assembly process takes longer – and time is money. Increasingly, companies assembling boards want to use only a single soldering process – reflow soldering. PIP makes it possible to solder PTH and SMT parts at the same time. This does mean that PTH parts housings need to be made in high-temperature-resistant plastics, but despite this, an overall cost reduction at board level can be achieved by eliminating an entire assembly stage. This trend is likely to lead to greater use of high-performance plastics such as PA4T and PA46.

Bio-Based High-Temperature Polyamides

To push the performance envelope even further, DSM has recently launched a new copolymer called ForTii Eco, with flow properties 30% better than the original ForTii. With improved robustness, ForTii Eco enables even greater component miniaturization. In addition, material processability during injection moulding has been significantly improved to make it ideal for product designers and easy to handle for moulders.

Environmental sustainability, often an issue addressed because of pressure from consumer groups, has evolved into a serious business opportunity for manufacturers and their suppliers. "Green design" innovations help reduce the environmental impact of products during manufacture and in use. Renewable polymers help save on consumption of resources such as mineral oil and reduce carbon dioxide emissions.

The use of renewable materials in ForTii Eco can be important in helping producers of various electronic equipment to obtain basic bronze EPEAT certification as well as higher silver and gold ratings under the EPEAT global rating system. Up to 95% of technical products at governmental institutions in the US now need to be EPEAT certified, which means that EPEAT has become a serious business driver for OEMs.

For a product to achieve a bronze rating, it needs to meet 22 criteria in eight performance categories, which are:

- Reduction or elimination of environmentally-sensitive materials, including certain flame retardants;
- Materials selection, which also covers use of recycled materials and renewables;
- Design for end-of-life;
- Product longevity/lifecycle extension;
- Energy conservation;
- End-of-life management;
- Corporate performance;
- Packaging.

For silver, a product has to meet all the compulsory criteria plus at least 16 optional ones; and to obtain the gold rating, it must meet all required criteria as well as at least 25 optional criteria. So an EPEAT rating beyond the basic bronze requires strategic considerations of which plastics to use in electronic components.

The ForTii Eco grades have a bio-content ranging from 10-25% by weight on a compound basis. The first three in the family are ForTii Eco E61, ForTii Eco E11 and ForTii Eco LDS62. Key applications for ForTii Eco E11 and ForTii Eco E61 include SMT connectors like USB Type-C or audio jacks; ForTii Eco LDS62 is highly suitable for antennas, RFID security casings for smart payments and switches and sensors in various segments, ranging from medical to automotive.

Bio-based PA4T grades have an elongation at break of between 2.3% and 2.5%, depending on the flame retardant used, which means that they have sufficient ductility for use in snap-fit parts and parts with extremely thin walls. Prototype audio jacks moulded in ForTii Eco E61 for example do not crack after undergoing extensive mechanical testing that involves insertion and extraction of the jack in its socket.

The next generation of audio jacks may require use of the improved flow properties of the new materials. This is because audio jacks located along the sides of mobile phones are the limiting factor on how thin the phones can be made. Use of higher flow materials will make it possible to make the jacks smaller.

ForTii Eco grades have a further advantage: they leave lower deposits on moulds at optimal processing temperatures, making it possible to extend mould maintenance intervals by about twofold. Given that in production of some parts it is currently necessary to clean moulds every two or three days – and in some extreme cases at the end of every shift – this can considerably boost productivity.

3D-MIDs

The ForTii Eco LDS62 grade is an ideal material, especially for the production of 3D Moulded Interconnect Devices (3D-MIDs); antennas for mobile electronics are a typical example. This product contains a special additive that enables incorporation onto the surface of the part of very fine and precise electrical circuitry by highly cost-effective laser direct soldering (LDS). 3D-MID technology is now of increasing importance for automotive electronics and also in white goods as the Internet of Things begins to take shape.

PUSHING THE LIMITS

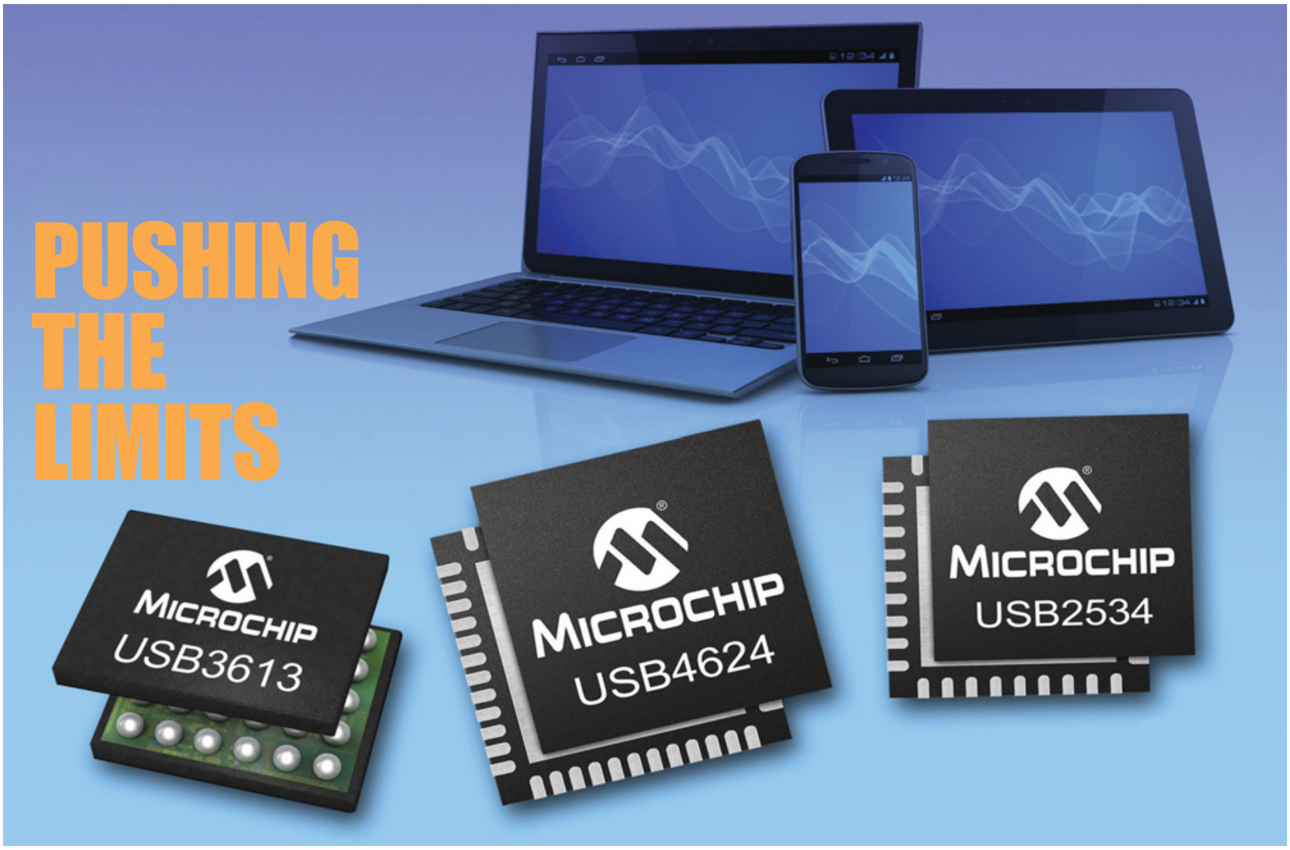

TECHNICAL AUTHORS FROM MICROCHIP EXPLAIN HOW THE USB CURRENT LIMIT CAN BE INCREASED TO MORE EFFICIENTLY CHARGE PORTABLE DEVICES

Universal Serial Bus (USB) is the most used computer interface in the world. It started as an expansion bus for personal computers (PCs), but proliferated quickly due to its flexibility, performance and hot-plug capability. Most portable electronic devices that require PC connectivity use USB for file transfers, including MP3 players, digital cameras, mobile phones and tablets.

Since a standard USB bus downstream port can provide at least 500mA (USB 2.0) or 900mA (USB 3.0) of current, it became convenient for charging such devices. But if this current limit was to increase, charging could become even more efficient. One way to achieve this is with the Microchip USB2534 hub controller using RapidCharge.

If the current required exceeds the limits then both the charging device and charging port must follow a protocol to enable battery charging. A downstream battery-charging port is responsible for providing proper handshake signalling to the charging device to indicate it's been connected to a charging port and to draw current above the standard USB limits.

The signalling varies depending on the portable device. Some portable devices follow USB-IF BC1.2 protocols, but there is an installed base of devices that use proprietary handshake protocols for battery charging, known as legacy modes.

Legacy devices support some form of battery-charging detection intended for use with a dedicated charger. Some of these chargers short D+ to D- directly or connect them through a series resistor. For charger detection, some legacy devices apply a voltage on D+ by connecting a pull-up resistor and then sensing a voltage on D-. If a positive voltage is detected, the device can assume it is plugged into a dedicated charger and not a standard USB port.

Other devices pull down one data line while pulling the other up. Once the device detects a charger by the presence of a voltage on D-, it can start charging from the V_{bus} connection at current levels that exceed the USB specification.

Other legacy devices rely on the charger to drive fixed voltages (more than 1V) on the D+ and D- data lines. These are referred to as SE1 chargers. If these voltages are sensed by the charging device, the device assumes it is plugged into a dedicated charger and starts charging. A standard USB downstream port would not present these fixed voltages on the D+ and D- lines.

Charger Detection

The portable device is responsible for charger detection; Figure 1 shows the hardware.

There are five functional blocks shown in Figure 1: V_{bus} detect, data contact detect, primary detection, secondary detection and ACA detection. A portable device includes a session-valid comparator. V_{bus} must be above the threshold voltage before charger detection is initiated. This is shown as $V_{OTG\_SESS\_VLD}$ on the diagram.

Data contact detect is an optional block used to confirm that the data lines made contact during attachment. A current source on D+ and a pull-down resistor on D- are turned on. If the D+ line goes low this indicates that data lines are attached to a charging port or a standard port and the logic proceeds to start primary detection.

A timeout circuit is needed to ensure that primary detection starts after a set time following attachment, in case contact is not detected or the data contact detect block is not present.

A portable device is needed to implement primary detection, used to distinguish between a standard downstream port (SDP) and a charging port. Figure 2 shows what happens when the device is connected to a dedicated charging port (DCP), Figure 3 connected to a charging downstream port (CDP) and Figure 4 connected to an SDP.

Secondary detection is used to distinguish between a DCP and a CDP. If a portable device is ready for enumeration within a set time after V_{bus} detection, it can bypass secondary detection, otherwise it needs to implement it. Only portable devices with a USB Micro-AB connector can support ACA detection and thus it is optional. Detection is done by measuring the resistance of the ID pin.

Battery Charging

The Microchip USB2534 hub controller includes RapidCharge technology for providing proper handshake signalling to portable devices on downstream ports for battery charging. It also does USB upstream battery charger detection.

To charge most portable devices, it is necessary to provide the proper handshake signals for legacy chargers, SE1 chargers, chargers compliant with Chinese Telecommunications Industry battery charger specification YD/T 1591-2009 and BC1.2 compliant devices. The hub controller includes all these protocols to implement complete battery charging supporting devices from Apple, Samsung and others.

If a USB downstream port is configured to support battery charging, the port is a CDP if it can enumerate the device or DCP if it can't. If the port is not configured to support battery charging, the port is an SDP.

The downstream ports can be enabled for battery charging by adding a pull-up resistor (10kΩ) on the battery charging configuration strap for the corresponding port. These straps are sampled at reset and if they are found high the corresponding port is enabled for battery charging.

Battery charging can also be enabled with the battery-charging configuration registers in the USB2534. These configuration registers are used by the internal ROM firmware to configure the battery charging functionality for each port. These registers can be modified by a configuration programmed in the one time programmable (OTP) memory using the ProTouch programming tool.

The ProTouch tool is a Microchip-developed tool for configuration and programming of the USB2534 hub controller. It can be used for development and prototyping where a single part is programmed, or for multiple parts in a manufacturing environment.

When there is no upstream V_{bus}, and consequently no USB host connected on the upstream port, the downstream battery-charging-enabled ports will operate as DCP ports. These ports will exit this mode if the upstream port has a host connection. DCP mode will also be entered if the USB2534 is suspended and remote wakeup disabled.

In DCP-mode battery charging, the port will attempt to handshake with and identify the BC capable device. In DCP mode the device always starts in SE1 mode. It cannot detect that an SE1 device is

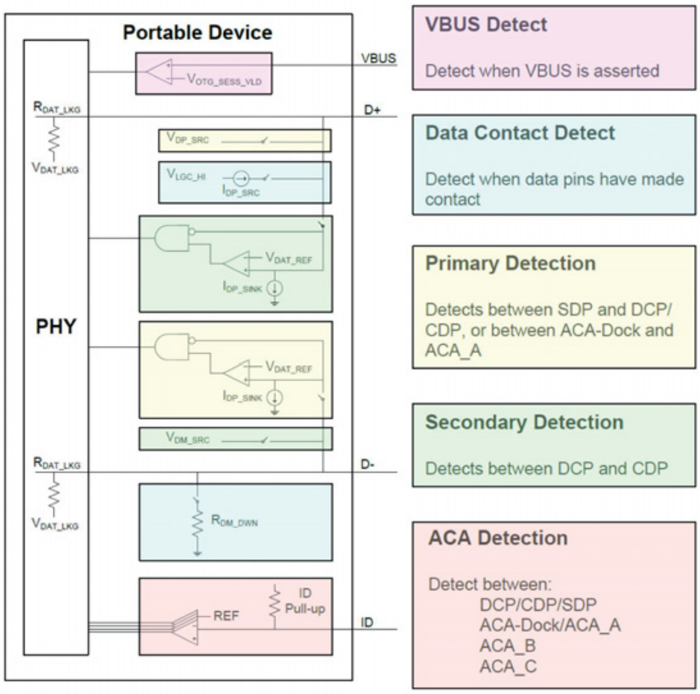

Figure 1: Charger detection hardware

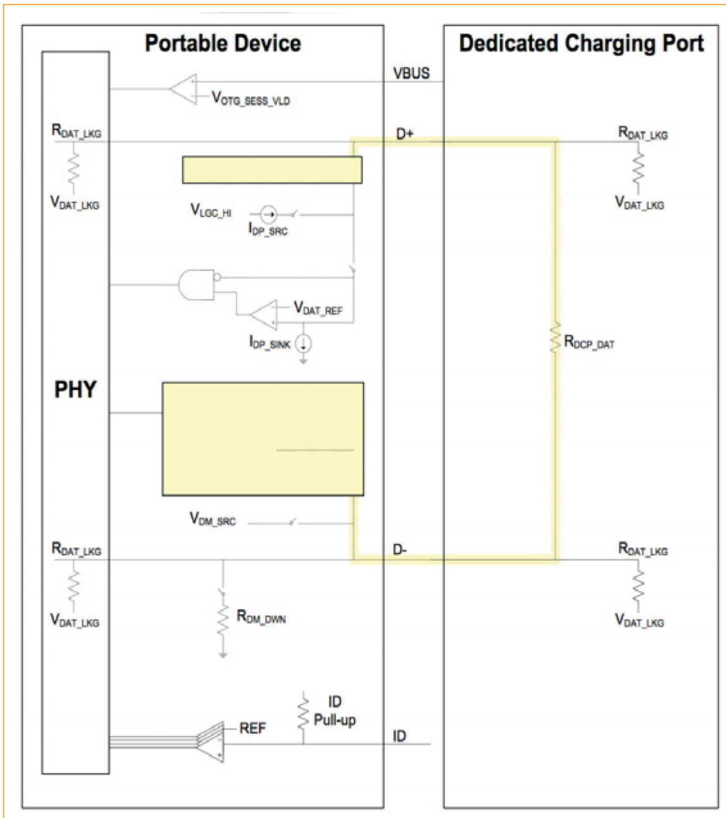

Figure 2: Primary detection with dedicated charging port

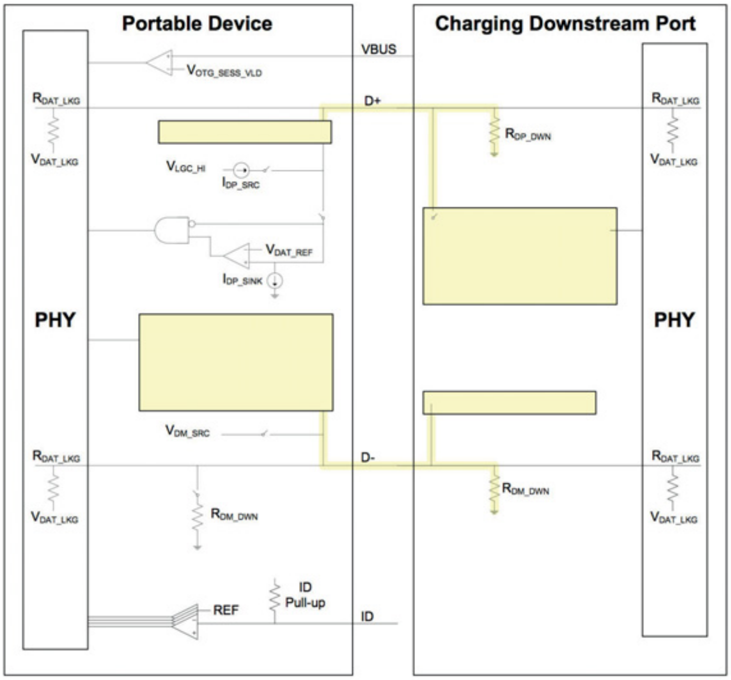

Figure 3: Primary detection with a charging downstream port

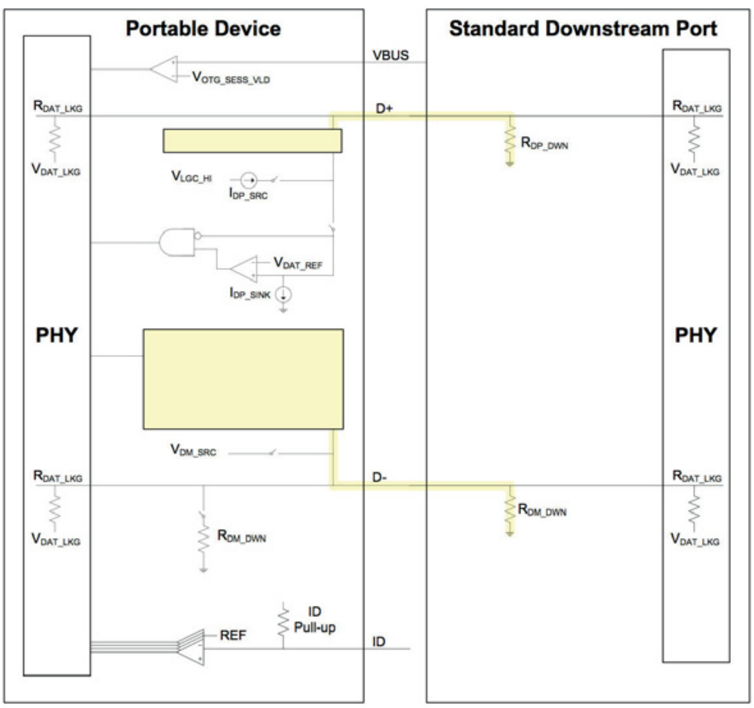

Figure 4: Primary detection with standard downstream port

attached, but it can detect that a non-SE1 device is attached when the device toggles DM or DP.

Upon entering RapidCharge mode, the USB2534 goes into SE1 charging mode and the port presents the SE1 voltage levels. If an SE1 device is attached, it will passively detect the SE1 levels and begin to charge. The DCP will not be able to detect the presence of the SE1 device. The port remains in SE1 charging mode while the SE1 PD charges.

If a BC 1.2 device is attached, its current is strong enough to pull the D- line low. Likewise, legacy charging devices have been observed to pull the D- line low when attached. To accommodate this, the downstream port transitions to legacy charging mode if the classic D- line state is detected as low. The D- line state is de-bounced to avoid false detects from device plug-ins. Legacy charging mode is shown in Figure 5.

The battery-charging-enabled ports will exit DCP mode and enter CDP mode if the upstream port gets a host connection. On detection of the USB host set address command, any BC enabled port will be turned off for at least 250ms before it can be turned on, to allow the port power to decay. If the host sends a command to turn on the port power, the command will be delayed appropriately. If the command is received after the timer has expired, it will be executed immediately.

An external MCU can override the automatic charger detection sequence by modifying the SMBus runtime battery-charging registers. Because the start of battery charging detection is set to occur by default, the MCU must write to the battery-charging control register or the configuration interlock register to disable the automatic sequence before the sequence begins. If the automatic sequence is disabled, the MCU can still initiate it manually.

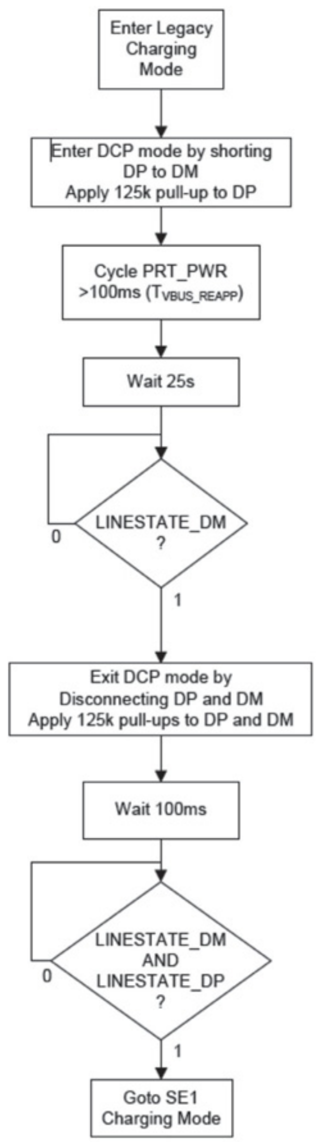

Figure 5: Legacy charging mode

Convenient Mechanism

USB battery charging provides a convenient mechanism for recharging batteries on portable devices such as mobile phones and tablets. The USB-IF published the BC1.2 battery-charging specification to help standardise protocols used between chargers and charging devices to safely enable battery charging. ●


RS
Realise your vision
We have all the parts you need to solve your technical challenges and bring your design projects to life.
Never get stuck again. Our extensive range of semiconductors, passives and interconnects has got you covered. With thousands of brands you know and trust, you can count on us for the best solution.
Find the right parts at
uk.rs-online.com

A FREQUENTLY OVERLOOKED ASPECT OF USING SMARTPHONES AND OTHER PORTABLE DEVICES IS THEIR OPERATION AFTER BEING DROPPED IN LIQUIDS. **JOHN KAVANAGH**, CHIEF CREATIVE OFFICER (CCO) OF REDUX EXPLORES

WATERPROOFING SMARTPHONES: WHAT TO DO?

No one reading this article will be surprised that younger people today have become increasingly attached to their mobile phones. Take-up of smartphones among the younger population continues to outpace the older generations, in some cases to the point of addiction. Perhaps as a result of this increased dependence on mobile devices, waterproofing is emerging as a key value-add for younger age groups.

Engineering company Redux recently commissioned research into the issue of waterproofing and found that 58% of those between the ages of 18-24 claim to have damaged a device by dropping it in water or by spilling liquid on it, compared to just 9% of over-55s.

This statistic is consistent with that of TSB Insurance, which recently revealed that customers make more claims due to water damage than any other type of problem. Water damage accounts for 23% of mobile phone and 7% of laptop claims, according to the insurer.

In Redux's survey, many respondents claim to have dropped their phone down the loo or in the bath. One unlucky respondent had even drowned multiple devices, including in the sink, in beer, in a pool, and a whole other assortment of watery graves.

Given the price of many of today's smartphones, it's perhaps no surprise that 18-24-year-olds want their devices to be more robust. After all, if a device is used multiple times per hour each day, durability will be key to a long lifespan.

Meeting Customer Needs

As analysts predict that the smartphone markets in developed regions will peak in the coming year, manufacturers are increasingly examining customer frustrations to identify where they should concentrate development efforts. As a result, device manufacturers have already begun to address the challenge of waterproofing their products.

The two most high-profile attempts currently on the market are the Samsung Galaxy and Sony Experia X. Both claim to be able to survive in water, having received IPX8 ratings to signify that they are safe from "immersion in water with a depth of more than 1 metre". To achieve this level of protection, Samsung and Sony have fitted bespoke rubber seals to all vents and inlets on the devices' external chassis, which prevent water from entering.

However, there are limitations to this approach, since these vents only provide real protection against immersion in fresh water. Corrosive elements in saline solutions, detergents, soaps and sugary liquids can dry out and erode the vents, rendering them less effective.

Long-term exposure to these conditions will ultimately destroy the waterproofing, making current methods only useful protection against one-off accidents. Similarly, few consumers will be willing to risk their device by cleaning out the rubber seals should they expose it to one of these liquids on an occasion, leaving corrosive residue behind.

Some devices on the market use more durable materials for the seals, which offer greater protection against non-freshwater liquids. There are also aftermarket waterproof sprays like Nanostate's Flash Flood that provide a durable coating to protect devices from moisture. The company claims that its spray forms a powerful barrier over the entire device, making it liquid and moisture resistant.

Taking this coating a stage further, some companies are exploring ways to make nano-coatings part of the manufacturing process of a device, so instead of waterproofing just the casing, individual components within the device would – in theory – be water tolerant. The cost of implementing this approach is so far hampering progress, however.

A Better Fix

Overall, none of these methods fix the fundamental flaw in the approach that, as long as devices rely upon vents and seals, there will always be some risk of ingress. The real solution is to remove the need for external vents and inlets completely, which on modern smartphones are typically the microphone and headphone ports, power sockets and speaker grilles.

The most straightforward of these vents to resolve is the microphone. By manufacturing the microphone's membrane and surrounding container out of a water-resistant material, this port can enjoy a watertight seal.

Designing out the headphone and power ports is also an entirely realistic challenge, as alternative, wireless connections are already included in the majority of leading smartphones on the market today. Practically, wireless charging pads and Bluetooth headphones will likely need much wider consumer penetration before manufacturers take the plunge and throw these physical ports out of their designs. Apple has already removed the headphone port from its new iPhone – a move that other manufacturers will no doubt follow suit.

> "Water damage accounts for 23% of mobile phone and 7% of laptop claims, according to the TSB Insurance

This leaves speaker grilles as the last remaining obstacle to waterproof smartphones. These grilles are essential for enabling sound generated by the micro speaker to exit the device, and any attempt to cover the grilles with a material will likely result in muffled sound output and, hence, poor audio performance.

Bending-Wave Technology

The clearest solution to the audio challenge would be to replace the micro-speaker entirely with bending-wave technology, which can generate sound from any hard surface, like the phone's flat touchscreen panel. This approach removes the need for audio grilles entirely.

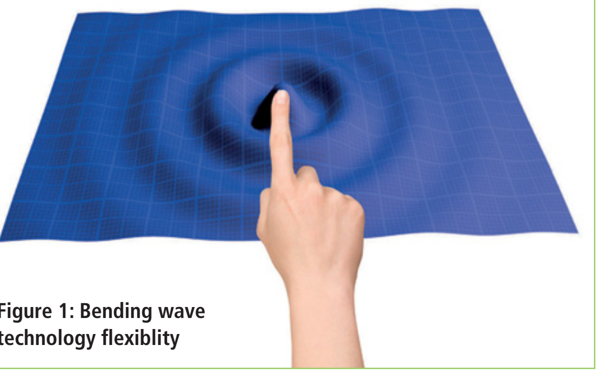

Figure 1: Bending wave technology flexiblity

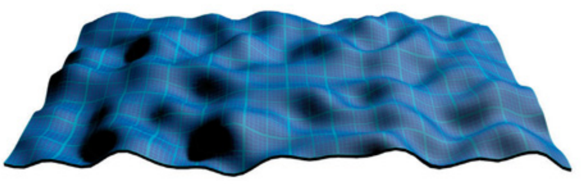

Figure 2: Bending wave technology

Bending-wave technology actuators are placed inside the body of the device, below the device's touchscreen panel. These generate dispersed modal waveforms that vibrate the surface to create audio. As a result, the entire screen of a smartphone can become the speaker, producing a much fuller, more natural sound. In fact, while traditional micro-speakers typically feature a lower frequency limit of around 700Hz, this bending-wave technology extends this lower limit by over one octave – important given that speech intelligibility requires an undistorted output over the 300Hz-8kHz range.

By taking these steps – using waterproof materials in microphones and wireless standards for power and headphone connectivity, introducing bending-wave technology to produce audio would result in a completely sealed, ingress-proofed design. Then, and only then, would it be fair to consider a device waterproof in the sense that consumers think of – i.e. capable of withstanding submergence in drinks, loos, bathtubs, swimming pools and other bodies of water.

What's more, the market dynamics forecasts suggest that manufacturers are only going to face an ever-more competitive market in securing mindshare among the population. To win an edge over competitors, they'll need to concentrate their efforts on adapting designs to solve the frustrations of the consumers that are most likely to be purchasing new devices.

Waterproofing devices is a clear route to achieving an edge, helping to mitigate a longstanding frustration among young mobile users, whilst simultaneously requiring manufacturers to adopt technologies that ultimately improve device functionality and performance. ●

Figure 1: Nowadays, consumers are increasingly expecting waterproof phones

MAKING A SPLASH WITH WATER-RESISTANT DIGITAL DEVICES

THE GROWING TREND OF WATERPROOFING PORTABLE ELECTRONIC DEVICES HAS LED FASTENER MANUFACTURERS TO DISCOVER A LOW-COST SOLUTION. BY **DOUG CLARK**, US-BASED TECHNICAL WRITER

The trend in consumer electronics has always been to make devices faster, smarter and with even more functionalities. But waterproofing has become the new focus of global electronics manufacturers, and most brands are rushing to get there fast to avoid being left behind in this ultra-competitive market.

Since water-resistant standards play a big role in making expensive handheld and wearable digital devices more durable, the industry has adopted the IPX7 rating, which protects against immersion in water for 30 minutes at a depth of 1 meter (3.28 feet). Yet the critical element in meeting or exceeding these higher standards is something most consumers are barely aware of – the micro fasteners that must lock out moisture while also fitting into the aesthetics of the phone, watch or tablet design. Making devices that are eye-catching as well as water-, air- and dust-proof adds incredible value to a new product.

Fulfilling both demands is proving difficult because some of the most effective processes for making large, practical screws are not suitable for micro fasteners, experts say. As a result, the cost per unit is two or three times higher for the smaller screws. In addition, in some cases overspray of the sealant needed to ensure water resistance has led to discoloration that ruins the appearance of the device's exterior.

Testing For A Solution

A solution that improves reliability while lowering costs was discovered using a variable-water-pressure simulation chamber, where a combination of water and air pressure simulates water depth of 1-10m.

The test was conducted according to guidelines set by the International Organization for Standardization (ISO) using a minimum of 32 pieces, in this case the M1.0 x 3, a common-sized screw used in digital devices.

Initially the screws were tightened to the correct seating torque specifications using a micro torque wrench. (ISO threads = 0.36kgf-cm; threads = 0.42kgf-cm. A 15% increase in torque was added to the threads in order to achieve the same clamp load due to friction.) Water pressure was applied to the head of each fastener to simulate an actual environment that could destroy a portable electronic device, such as a toilet, swimming pool or bathtub.

Once the chamber achieved full pressure, engineers set a timer for 30 minutes and then closely watched the pressure meter and checked for leaks in the dry bottom portion of the chamber. If the pressure dropped and/or water was found on the bottom testplate, this would indicate a system failure.

Exceeding IPX7 Standards, Reducing Costs

The test was created and executed by Sean Riskin, Director of Engineering for the Global Electronics Group at STANLEY Engineered Fastening. Afterward he created a revealing study that included his findings for nearly a dozen fastener configurations from various brands to find the best solutions that meet or exceed the IPX7 standards.

Most sealants for micro fasteners are a nylon- or Teflon-based substance and there are only two options for applying the protection. Manufacturers either seal the threads, or seal underneath the head of the screw; both have advantages and disadvantages.

Sealing just the threads may not protect the multiple layers of components in a typical fastened joint, because the components being fastened together are in the path of water before the protective sealant. Sealing under the head is preferable because the head is the first barrier against moisture. Yet, this is the method that in some cases results in overspray and discoloration caused by the application process.

"You don't want to spend two or three times as much on a fastener and not have it look cosmetically pleasing," said Riskin. "In a sense, electronic manufacturers are struggling with a three-way battle: function versus beauty versus cost."

Also, the sealant is prohibitively costly because it must be applied to every single unit as a secondary operation, forcing major manufacturers to spend upwards of tens of millions of dollars annually on micro fasteners alone.

Suitable Solutions

What if the sealant could be eliminated? That, however, may be easier said than done.

The sealant creates a water and dust barrier and, in addition, each screw must have an anti-vibration feature so it won't loosen and back out during normal use of the device. Both features are second and third operations that add a lot to the overall price of a fastener.

The solution Riskin was looking for came from the combination of under-head design features of screws and an innovation by Spiralock, a subsidiary of STANLEY, which years ago re-engineered a female thread profile that adds a unique 30-degree wedge ramp at the root of the thread and mates with standard 60-degree male fasteners. This innovation removes the need for nylon-based patches or other anti-vibration countermeasures and therefore significantly reduces the cost of fasteners.

Riskin's study revealed other advantages. When torqued to specifications, standard screws are not perfectly perpendicular; most are a couple of degrees off-access, effectively providing a gap where fluid can enter.

The Spiralock thread profile in comparison is self-centering and the head of the fastener is perpendicular to the bearing surface. Riskin knew that this alone would not entirely seal out moisture, so he added an 87-degree under-head feature and semi-flat head to the micro fasteners. Although the head designs have been available for years, this is the first time they've been combined with Spiralock's modified locking thread profile to create excellent moisture sealing joints that exceed the IPX7 rating standards. It also creates a vibration-proof joint that is easy to assemble, saving brands time and money.

> "The sealant is prohibitively costly because it must be applied to every single unit as a secondary operation, forcing major manufacturers to spend upwards of tens of millions of dollars annually on micro fasteners alone

"When you're stacking multiple components for assembly, tolerances always add up and nothing is perfect. So more bearing surface area can be a major advantage. These solutions provide additional bearing surface area or a single circular point of contact under the head, significantly improving the sealing surface," said Riskin.

Now that his study is complete, Riskin hopes his discoveries will present handheld and wearable device manufacturers with new possibilities.

"Nobody wants to be just as good as their competition; they want to be better! Everyone is trying to get a piece of the market by diversifying themselves. That's exciting. Imagine what we might be buying and wearing in a couple years," he added. ●

Figure 2: Spiralock IPX7 fastener

NOVEL PROTECTION DESIGN FOR PORTABLE DEVICES

QINLONG CUI, LIANJIANG LI, SHUTING WANG AND **LAN HONG** FROM NORTHEASTERN UNIVERSITY, QINHUANGDAO, AND **WEN CAO** FROM XI'AN INTERNATIONAL STUDIES UNIVERSITY, CHINA, ANALYZE THE DAMAGE PORTABLE DEVICES SUSTAIN WHEN DROPPED, AND PRESENT A NEW PROTECTION METHOD

The popularity of smart mobile devices seems to be unstoppable due to the functionalities they provide and their ease of use, including touchscreens rather than the traditional, button-type interfaces.

As early as 2007, after Steve Jobs returned to Apple, the first generation of iPhones had only one primary button and a touchscreen, and much smaller dimensions and better screen proportions. And with the advent of 3G and 4G networks that can carry streaming video, the portable devices' screens grew bigger yet again.

In addition, for aesthetics, mobile device makers keep changing the appearance of mobile phones: shells have moved away from traditional plastic to metal and glass. Apple devices like the iPhone and iPad are all glass in front and metal on the back. Samsung's devices such as the Galaxy and Note use the same design concept, which improves efficiencies and user experience but also poses greater risk of damage.

To solve this problem, mobile device makers have adjusted the glass manufacturing processes and materials, for example by using Corning Gorilla Glass or Sapphire screens. Gorilla Glass has improved over several generations, in terms of its strength and susceptibility to slide marks, but its high cost makes it suitable only for middle-to-high-grade mobile devices.

Alhough mobile device makers continue to improve their products at different levels, their protection goes only so far, and mostly when devices are used in normal circumstances. Yet, devices being dropped and suffering from impacts are a daily headache for consumers, with significant – and in some cases irreparable – damage to screens and system innards. To protect these vulnerable devices, consumers often engulf their mobile phones in protective shells, creating a booming side market.

Novel Protection Methods

We've analyzed the impact of shell-protected mobile phones and found that if a phone falls flat on the ground, there's a large contact area, so the force of the impact spreads out. But if a phone falls on an edge or corner, the shell offers little protection. Protective shells also increase the device's overall size and alter its shape, which goes against the carefully thought-out design processes based on ergonomics, ease of use, functionality and aesthetics.

Some large companies have gone even further with their protection and have launched their own intelligent protection concepts, such as Amazon with its recoil shells and Honda with its airbag shells. The Amazon approach works by combining software-enabled status indicators and real-time fall detection with a mobile gravity acceleration sensor. On collision the software determines if the impact is beyond the damage threshold; if yes, six shells on the gas nozzle jet deploy to change the device's falling position (see Figure 1, left side) and reduce the rate of descent and/or soften the impact.

Although this invention can prevent damage to portable devices, there are still some unresolved issues, including:

● A hard shell can worsen hard landing. In the case of a hard

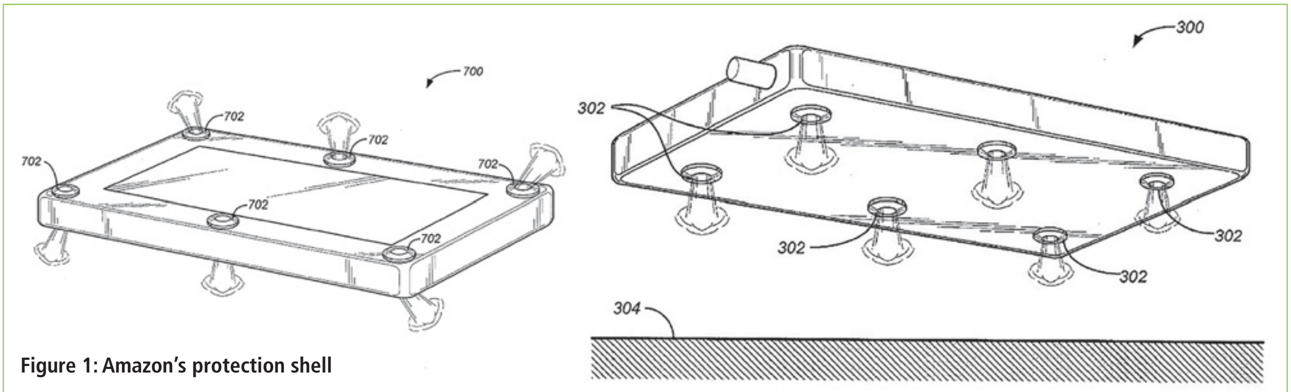

Figure 1: Amazon's protection shell

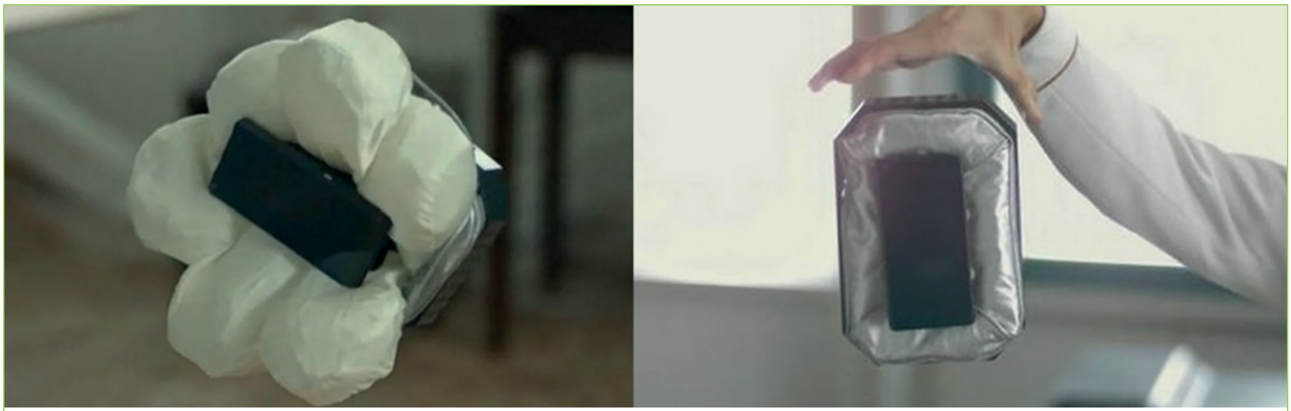

Figure 2: Honda-designed smartphone case N

surface (such as a concrete floor, for example), the portable device and its shell will damage more readily.

- The shell changes the device's general appearance.
- If the mobile device is placed inside apparel or bags for example, and if that bag is dropped, the shell no longer functions properly, as it cannot adjust within the space.
- The recoil gas requires a lot of energy to deploy and is an unrepeatable method. In addition it takes a long time for it to initially charge.

Honda's Solution

The mobile gravity-acceleration-sensor-based protection by Honda uses traditional car airbags, but is still in the laboratory. Most of our information is gathered from a YouTube video released by the company.

When a fall is detected, the shell releases gas to inflate an airbag; see Figure 2.

This method also suffers from shortfalls, including:

- The shell and its equipment make the device much bigger and more cumbersome.
- As with Amazon's method, this protection is more suited to direct falls rather than when the device is inside garments and bags.
- The inflating process and quantity of gas are not controlled – once airbags are inflated, they inflate fully. Although they provide soft landing, if during a fall other objects are hit first, this causes further bounces.
- The airbag cannot be withdrawn easily following inflation, and it cannot be reused.

Other Options

We've analyzed these issues and came up with the following steps to resolve them:

- Mathematical modeling of mobile devices in fall; analyzing factors such as initial height and speed and the effect they have on a device upon impact.
- A new mobile equipment protection system.
- Analyzing the new system's commercial feasibility.

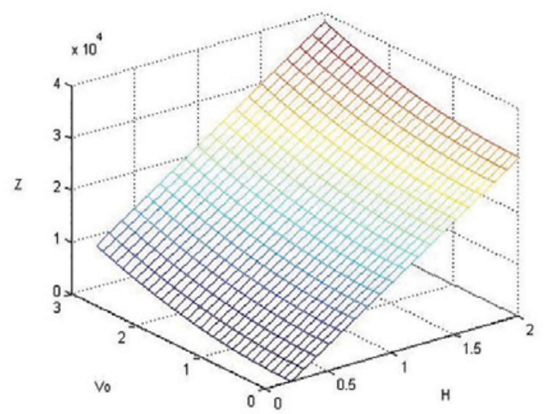

Figure 3: Damage to portable equipment without protection; H, the initial height; V_0, the initial velocity; Z, damage caused

PARTS	NAME	CLASSIFICATION	QUANTITY
ADDED PARTS	Airbags		18
	Storage tank		1
	Pipes	The tree gas pipeline	6
		Conjoined exhaust pipeline	1
		Conjoined inflate pipeline	1
	Electric control valve	Pneumatic valve	1
		The exhaust valve	1
	Liquid injection valve		1
	Check valve		18
EXISTING PARTS	CPU		1
	Acceleration sensor		1
	Control with the application		1
OTHERS	CO2 inject fluid		1

Table 1: Hardware components

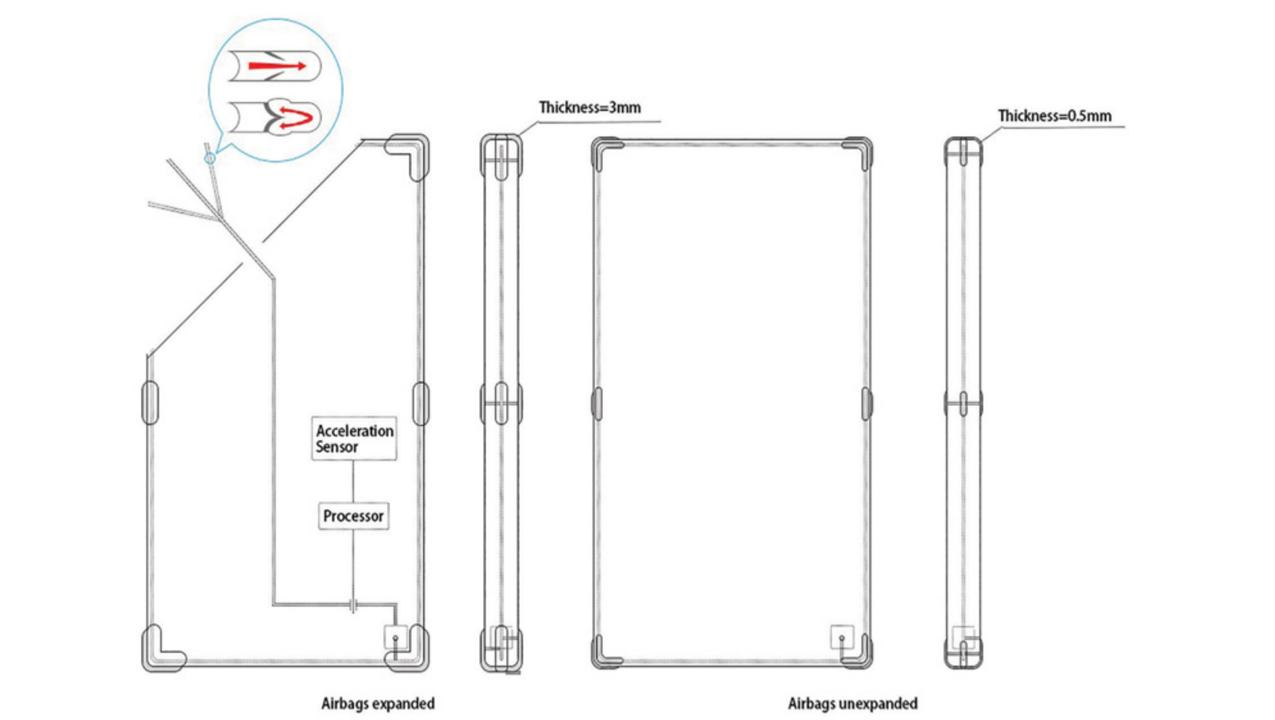

Figure 4: Protective system design

Figure 5: The ideal positioning of airbags

- Analyzing the theoretical and experimental results, and the follow-up steps needed for commercialization.

We analyzed the damage of mobile devices by using simple definitions and formulating a hypothesis with the support of Newtonian mechanics.

We've taken the initial height before fall to be H, initial velocity before fall V_o and acceleration affected by gravity G. The impact velocity of the portable device is given by:

$$V_T = \sqrt{2HG - v_0^2} \tag{1}$$

According to the law of momentum conservation, it can be defined as:

$$F\times(\mu_1 + \mu_2 + \mu_3) = \frac{1}{2}MV_T^2 \tag{2}$$

where F is the average collision impact, M is the device's mass and µ1, µ2 and µ3 are the deformation of the airbag, shell and ground at contact, respectively.

If the coefficient of the attitude angle fall to ground is A, the stress threshold is B, the damage rate (Z) following the fall can be defined as:

$$Z = F - A\times B \tag{3}$$

Or:

$$Z = \frac{M(HG - \frac{v_0^2}{2})}{\mu_1 + \mu_2 + \mu_3} - A\times B \tag{4}$$

According to our experiments, when a portable electronic device falls on a corner first, because of the small contact area, the pressure per unit area is much larger than when it falls flat on its surface.

In our experiments we used an iPhone 6 and found that if it fell freely from a 20cm height on one of its corners first, the phone or its shell did not suffer from any obvious damage.

Assuming that $\mu 3 \approx 0$, $\mu 2 = 0.1$mm, $\mu 1 = 0$, from M = 0.172kg, H = 0.2m, G = 9.8m/s², $V_o = 0$, using the equations of Table 1 we find that the stress threshold B = 3371.2.

We then created an analytical model to analyze the degree of damage Z dependent on the different heights H and initial velocities V_o; see Figure 3.

From the figure it can be seen that at initial velocity and height, the mobile device has the greatest kinetic energy just before it hits the ground, with its hard-material shell increasing the risk of damage. From the equation

$$Z = \frac{M(HG - \frac{v_0^2}{2})}{\mu_1 + \mu_2 + \mu_3} - A \times B$$

it can be determined that the greater the degree of plastic deformation the greater the damage.

Proposed Protection Design

Through experiments, we designed a protective system (see Figure 4) for portable devices based on an acceleration sensor and analog-to-digital converters (ADCs) for data acquisition, controlled with software installed in the device's own memory and run by the device's own processor, for example the A10 in the iPhone 6s. The full system component list is shown in Table 1.

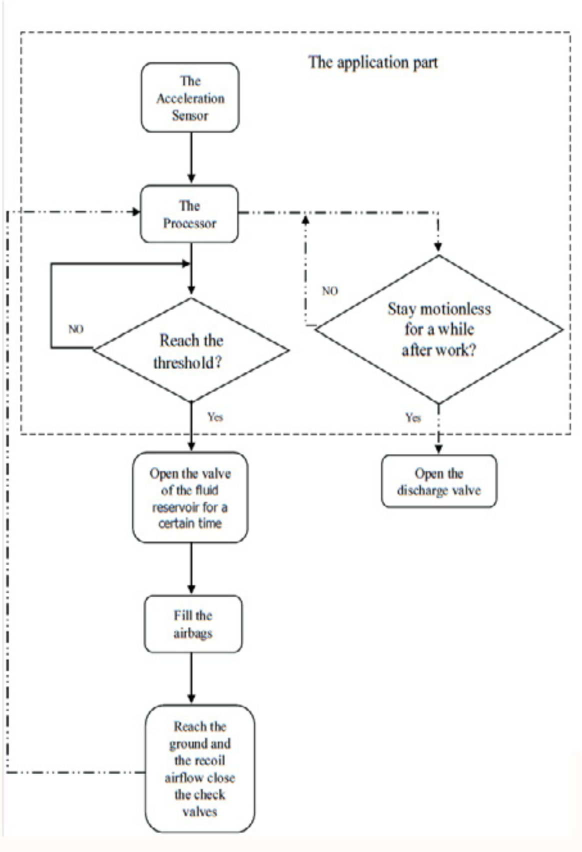

Figure 6: Monitor and control flow chart

System Operation

The system fits inside the portable device, using the device's own acceleration sensors, transducers and processors. The protective system will be fitted by the OEMs themselves at the outset, to accommodate the necessary components, such as gas pipes, tanks, miniature control valves and airbags.

As Figures 4 and 5 show, four airbags are arranged on the corners of the device, with two others centred on each long side, protecting the back and front of the device. Unlike normal airbags which typically use nylon-66 as their core material, our airbags are made of silicone, which is hard-wearing, flexible, inexpensive and thin. Other new materials with even better features are also feasible.

There are three kinds of pipes we designed to meet all operational demands. The conjoined inflate pipe line, controlled by the device's main CPU, is of bigger diameter to transport the gas needed for the system. The three smaller gas pipelines distribute gas to the airbags, with diameter large enough for fast airbag inflation. They have also been designed such that in case an airbag loses its gas a nearby one will inflate quickly without loss of function.

> "Devices being dropped and suffering from impacts are a daily headache for consumers, with significant – and in some cases irreparable – damage to screens and system innards

The conjoined exhaust pipelines are the most complex, needing the processor to control the miniature valves. Nevertheless, they too have been designed to be very small and take up little room in the portable device.

The installed real-time software is also of significance, even though its power and memory footprints are small. Acceleration sensors exist in most contemporary portable devices, which work continuously when, for example, the screen is turned on its side, or in navigation applications and games. The only controlled parts are the miniature electronic valves, but here the gasification is also a low energy-consuming process and only works when the protection system is activated. After landing, the program opens the exhaust valves to deflate the silicone airbags, which fold back to their original size. The system then resets for the next impact.

The Software

When the mobile device falls, the acceleration sensor will detect the corresponding acceleration A and velocity V. The processor then determines the acceleration and direction of the fall, $A = G$, $V > V_o$. If the data reflects potential damage over the threshold level, the processor opens the electric control valve of the liquid storage tank, releasing the gas – we recommend liquid CO2, as it's non-flammable, stable, cheap

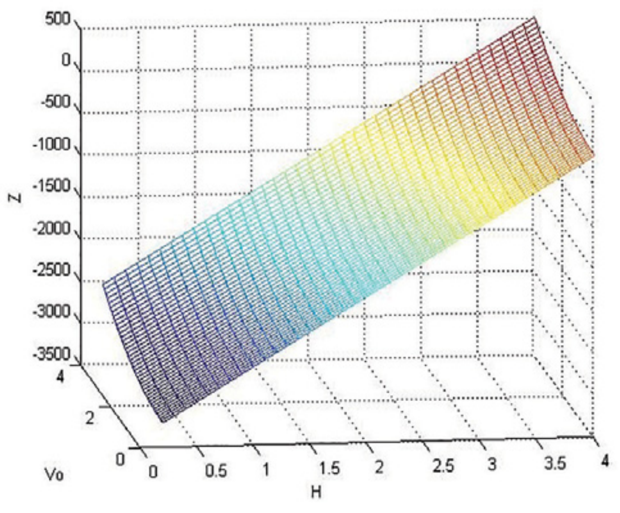

Figure 7: Model of the damage to a mobile phone with our protection installed. Initial height H, initial velocity V_0, damage caused Z

and environment-friendly. After landing, A = 0, V = 0.

When the numerical values are stable for a period of time, the exhaust valve will open automatically to deflate the airbags and arm them for the next fall.

After several inflation/deflation actions, if the liquid storage tank is empty, it can be topped up through the valve. This can be achieved easily by the users themselves by accessing the valve situated at the edge of their device, with an injection from a bottle of liquefied gas, akin to refueling old-fashioned gas lighters.

The modeling analysis of mobile equipment damage is shown in Figure 7, showing significantly decreased damage to the phone.

We determined that a portable device can be protected with this method from a fall of up to 4m, but not if it falls from a height of less than 20cm.

The system costs less than $20. Its layout won't affect the normal use of a portable device; it offers balanced weight and an even rate of airbags inflation and deflation. The system is especially suitable for high-end mobile devices, which keep getting lighter and thinner. ●


ODU-MAC®
THE ALL-ROUND SOLUTION FOR MANUAL MATING AND AUTOMATIC DOCKING
The intelligent path to customer-specific connections: ODU-MAC – our versatile modular connector solution enables the transmission of power, high current, high voltage, coax, high-speed data, fiber optics and other media such as air or fluid.
For your made-to-measure connection.
Compact modular connector system
Fail-safe performance thanks to outstanding contact reliability
6 standard docking solutions
High packing density
30 different high-speed inserts in the field of data technology
Up to 100,000 mating cycles
Stable low contact resistance
30 YEARS ODU-MAC® 2016
ODU-UK Ltd.
Phone: +44 1509 266433
sales@odu-uk.co.uk
www.odu-uk.co.uk
ODU®
A PERFECT ALLIANCE.

SECURING DATA ON THE IOT

SECURITY FEARS ARE A MAJOR BARRIER TO THE ADOPTION OF IOT. FORTUNATELY, IT IS BECOMING EASIER TO BUILD ROBUST SECURITY INTO IOT APPLICATIONS, FROM THE VERY BEGINNING. BY **ANDREW POCKSON**, DIVISIONAL MARKETING MANAGER AT ANGLIA COMPONENTS

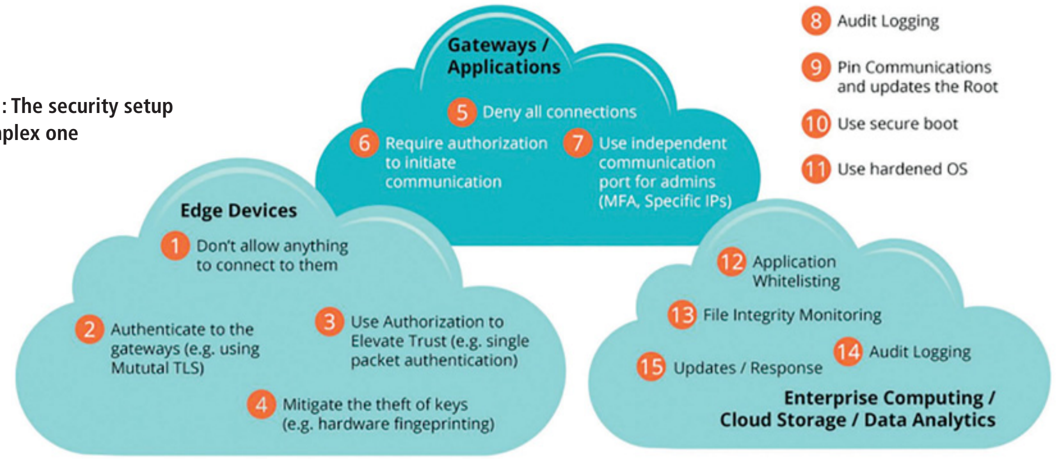

Figure 1: The security setup is a complex one

In the early days of the Internet of Things (IoT), security was an afterthought: time-to-market was always the first and most important consideration. But the sheer pace and complexity of IoT growth, coupled with the increasing agility and ingenuity of cybercriminals, has highlighted the pivotal role of security.

When HP Labs carried out a study of popular IoT devices in 2014, it found their security was appalling. This analysis of ten devices scrutinised end-to-end security capabilities including privacy protection, authorisation, encryption, user interface protection and code security. Around 70% of the devices revealed one or more significant vulnerabilities; over 250 vulnerabilities were found in total – an average of 25 per device.

Further high-profile reports have identified potentially dangerous vulnerabilities and exploits in IoT devices, from baby monitors and consumer wearables, to Internet-connected vehicles and medical equipment. Poor security in any device could potentially compromise the whole system, including industrial facilities, government and financial organisations, data centres and network infrastructure. Security needs to be built in from the start.

Fortunately, designers do not have to compromise time-to-market in order to integrate robust security standards into new devices. Turnkey hardware solutions allow security to be built in from the start of a new design. A further advantage is that new designs can be brought to market without investing in extensive security expertise. Host software libraries, demonstration and prototyping tools take care of that. Secure elements such as STSAFE-A from STMicro and Gemalto's Cinterion are prime examples of this approach.

Secure Elements

The STSAFE-A100 by STMicroelectronics is a highly secure solution that provides authentication and data management services to a local or remote host. It consists of a full turnkey IC with a secure operating system that runs on the latest generation of secure microcontrollers. Certification to Common Criteria EAL5+ provides banking-level security that meets industry standards.

> "Poor security in any device could potentially compromise the whole system, including industrial facilities, government and financial organisations, data centres and network infrastructure

When used in an IoT device, the chip connects to the local host via its I2C-bus slave interface, enabling transmission up to 400kbps with true open-drain pads and 7-bit addressing. It then authenticates with a remote host using the local host as a pass-through to the remote server. It proves to remote or local hosts that a certain peripheral or IoT device is legitimate. Manufacturers can therefore control which peripherals are permissible to use in conjunction with the original equipment. Secure elements can also be used by service providers to ensure specific services are only provided to IoT devices allowed to use them.

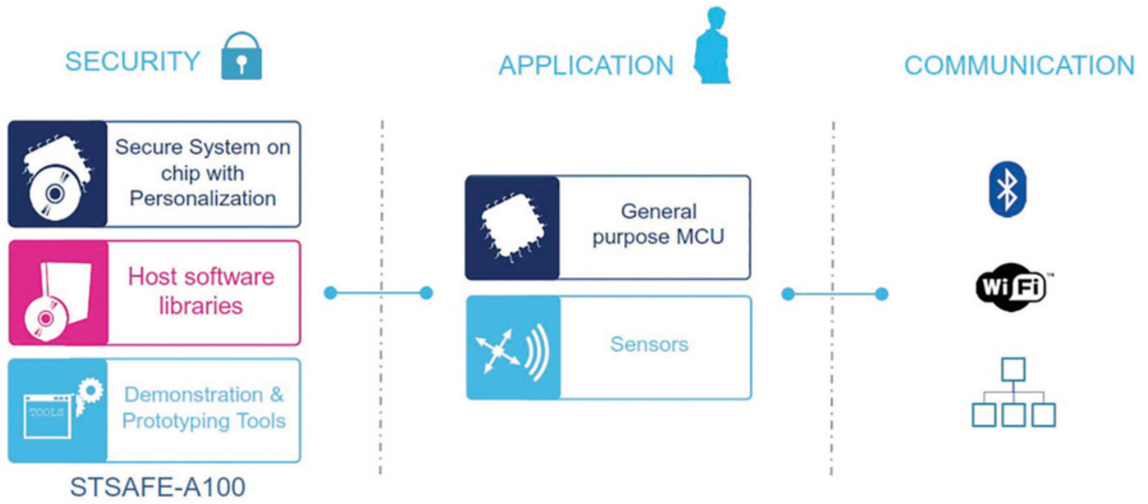

Figure 2: Secure IoT development is accelerated by secure elements with host software libraries, demonstration and prototyping tools

Authentication is secured using advanced asymmetric cryptography, and digital signatures are generated with elliptic curve digital signature algorithm (ECDSA) schemes with SHA-256 and SHA-384. The secure element is also compatible with USB Type-C authentication.

Communication with a remote host is secured via Transport Layer Security (TLS) handshaking. Secure elements furthermore support the secure update of local hosts. With STSAFE, firmware updates benefit from its signature verification capabilities. Using public keys provided by the local host offloads the task from local application processors that have limited computing power and no ECC accelerator.

Where it is necessary to secure the exchange of sensitive information with the local host via I2C port, a secure channel can be set up based on AES-128-bit keys. Secure elements like the STSAFE-A100 can also be used to encrypt or decrypt data between the remote host and the local host.

Security With Lifecycle Management

Secure elements can be integrated with a comprehensive end-to-end security ecosystem that runs from IoT devices to infrastructures. This concept is exemplified by Gemalto's Cinterion Secure Element – a tamper-resistant hardware component that embeds in IoT and industrial equipment to deliver smartcard-level security and lifecycle management.

Smartcard-level security ensures that data is stored in a safe place and access granted only to authorised applications and people. The secure element enables over-the-air management of credentials as well as software updates.

Security at this level is not an afterthought. It must be incorporated from the ground up at the start of new development projects. Building security in from the outset is the only way to make the IoT safe and secure.

Solutions for application, data network and virtual machine encryption, signature management, cloud data security and enterprise key management are complemented by hardware security modules (HSMs) – dedicated crypto processors specifically designed for the protection of the crypto key lifecycle. These provide reliable protection for transactions, identities and applications by securing cryptographic keys and provisioning encryption, decryption, authentication and digital signing services.

SafeNet hardware security modules enable cryptographic operations to be offloaded to a dedicated cryptographic processor that eliminates bottlenecks and maximises application performance. Users can centralise lifecycle management of cryptographic keys – generation, distribution, rotation, storage, termination and archiving – in a purpose-built, highly secure appliance. ●

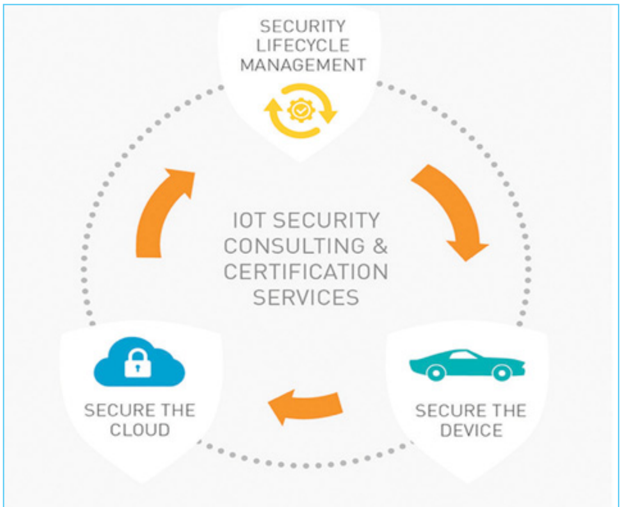

Figure 3: Secure elements like Gemalto Cinterion deliver lifecycle management in a comprehensive security ecosystem

AMPLIFIED NEGATIVE FEEDBACK CURRENT SOURCE AND VOLTAGE SOURCE

BY **MICHAEL KIWANUKA**, B.SC. (HONS) ELECTRONIC ENGINEERING

The amplified negative feedback (ANF) current source is a workhorse of discrete audio frequency amplifier design. This delightfully elegant little circuit can even be modified to function as a low impedance voltage source – the ANF voltage source – with the inclusion of a diode or two, an LED or a zener diode, as we will see here.

The ANF Current Source

Negative feedback in the ANF current source (see Figure 1) is series (current) derived, with the emitter current of transistor Q1 expressed as a feedback voltage by resistor R1. This voltage is amplified by the control transistor Q2 and applied, courtesy of Q2's collector, to the base of current source transistor Q1.

As far as the loop transmission path is concerned, current source transistor Q1 operates as an emitter follower, while control transistor Q2 operates as a common emitter stage. Biasing resistor R2 acts as the collector load of control transistor Q2.

The output impedance of a nominal current source may be simulated in SPICE by connecting the output of an ideal grounded independent voltage source to the output of the current source under test and running an AC analysis with respect to the voltage source. A plot is then obtained of the ratio of the voltage to the current at the current source's output.

The temptation to use an ideal independent current source to provide the test stimulus should be resisted; this is because an ideal current source possesses infinite output impedance and would therefore severely load the current source under test, giving erroneous results.

The increase in loop gain occasioned by amplification in common emitter control transistor Q2 gives the ANF current source more than ten times the output impedance at 100Hz (Figure 3) of the voltage-reference-biased current source of Figure 2, where no amplification of the feedback signal occurs. This result is confirmed by Camenzind in "*Designing Analog Chips*" and is contrary to Jung's counter-intuitive assertion in "*Sources 101: Audio Current Regulator Tests for High Performance Part 1: Basics of Operation*" that the output impedance of the voltage-reference-biased current source of Figure 2 is superior to that of the ANF current source. Indeed, the output impedance of the ANF current source is on a par with that of a cascode current source, being of the order of tens of megaohms rather than the tens of kilo-ohms suggested by Jung.

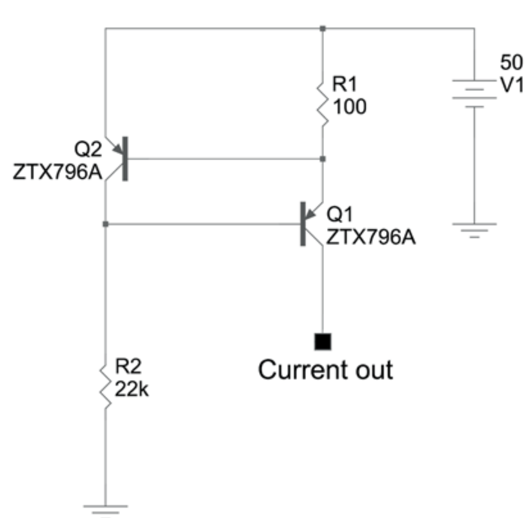

Figure 1: The amplified negative feedback current source

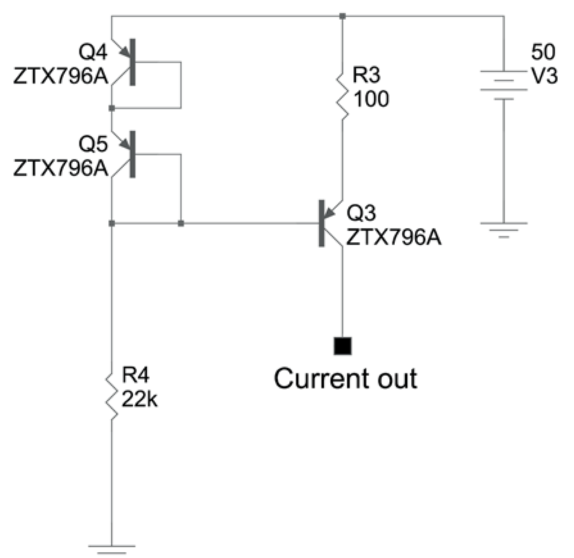

Figure 2: Voltage-reference-biased current source

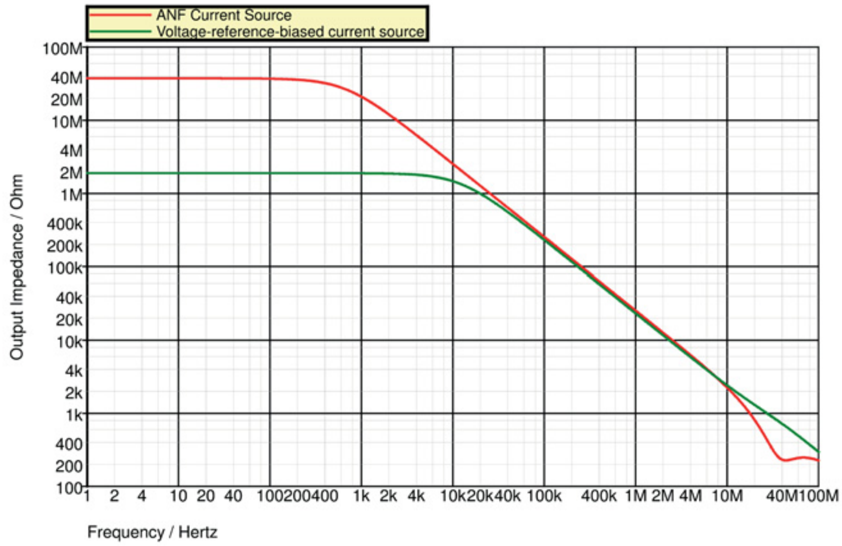

Figure 3: The output impedance of the ANF current source is superior to that of the voltage-reference-biased current source across the audio band

According To Jung…

Jung assumes that a current source's output impedance can be inferred from its power supply rejection ratio (PSRR), but this is incorrect precisely because the PSRR of the current sources of Figures 1 and 2 is as much a function of their associated biasing and decoupling components, if any, as their output impedance. For example, the PSRR of a current source can be increased independently and significantly, irrespective of its output impedance, by splitting its bias resistor into two and decoupling the midpoint of the two resistors to the supply rail (Figure 4).

Note that although the advantage with respect to output impedance of the ANF current source over the voltage-reference-biased current source typically extends across the audio band with most small signal transistors, this advantage disappears at ultrasonic frequencies. The output impedance of both current sources, and, indeed, all practical discrete-transistor current sources, drops at a single pole rate at high frequencies, due to parasitic capacitance to ground at the output (collector) of each current source.

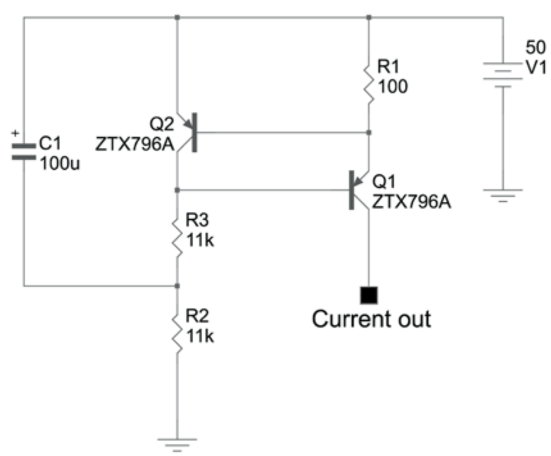

Figure 4: AC-decoupling the midpoint of bias resistors R2 and R3 increases the PSRR of the current source irrespective of its output impedance

Jung also maintains that the ANF current source is prone to oscillation if high bandwidth transistors are used in its construction; he recommends the inclusion of a small (~100Ω) resistor R3 in series with the control transistor's base to eliminate such oscillation (Figure 5).

To quantify the effect of this resistor on loop transmission, the ANF current source's feedback loop stability margins were evaluated with loop gain probes in LTspice. The loop gain probes may be inserted in series with the base of the control transistor (Figure 5) or in series with the base of the current source transistor.

Loop Gain Analysis

Depending on the current gain of the small signal transistors used, the ANF current source possesses 40dB~60dB loop gain or loop transmission at 100Hz. This relatively low loop gain, coupled with the low number and wide spacing of the feedback loop's singularities, would appear to preclude the possibility of instability. Nevertheless, loop gain analysis (Figure 6) indicates that the control transistor's base resistor improves loop gain stability margins by lowering the frequency of the dominant loop transmission pole which now comprises the input capacitance of the control transistor and its base resistor.

Loop gain analysis in LTspice also reveals that the value of the control transistor's base resistor R3 should be of the order of 1kΩ to effect a significant improvement in stability margins (Figure 6). If even greater margins of stability are required, then, in principle, a zero can be introduced in the vicinity of the unity loop gain frequency by connecting a small (~10pF) capacitor in parallel with the control transistor's base resistor.

Regrettably, this zero cannot be placed with an adequate degree of accuracy in practice because the input capacitance of the

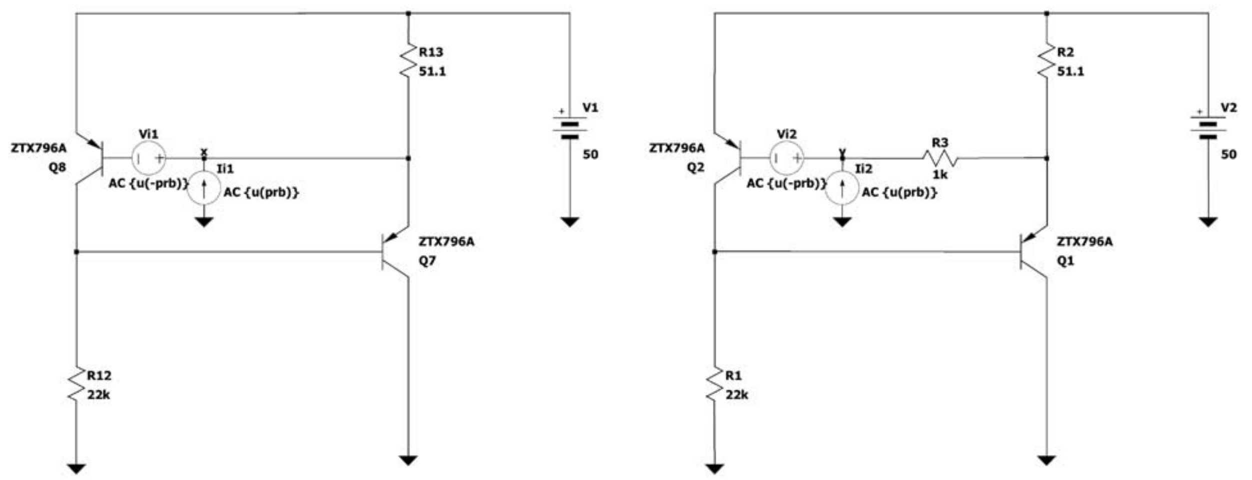

Figure 5: The loop gain probes are inserted in series with the base of the control transistors to obtain plots of loop transmission with frequency with and without a 1kΩ resistor in series with the base of the control transistors Q2 and Q8 respectively

control transistor, and, therefore, the unity loop gain frequency, is unknown and moreover varies widely from one transistor to another.

Increased freedom from unreliable transistor parameters may be achieved by using dominant pole-zero shunt compensation at the collector of the control transistor Q2 of the ANF current source (Figure 7); the shunt compensation network comprises capacitor C1 and resistor R3 connected between the collector of the control transistor Q2 and the supply rail, which is effectively at ground potential at the frequencies of interest.

Capacitor C1 lowers the frequency of the dominant loop transmission pole, while the small series resistor R3 introduces a zero in the vicinity of the unity loop gain frequency, improving phase margin from 28 degrees, without the compensation network, to 130 degrees (Figure 8); these singularities remain largely invariant, irrespective of the small signal transistors used, assuming the value of the control transistor's collector load resistor R2 remains constant. For values of the control transistor's collector load resistor R2 in the range 10kΩ~22kΩ, the values of the shunt compensation network's capacitor C1 and resistor R3 need not exceed 3.3nF and 10Ω respectively.

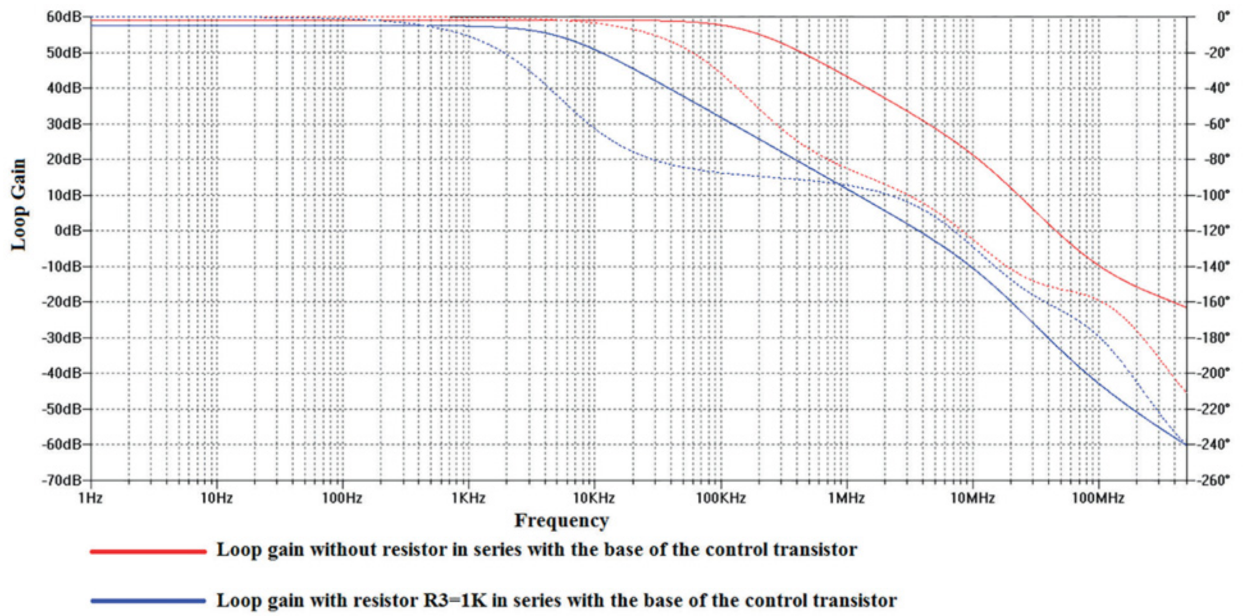

Figure 6: Phase margin improves from 28 degrees without a resistor in series with the base of the control transistor to 74 degrees with the 1K resistor in situ

The ANF Voltage Source

An ANF current source is easily converted into a low-impedance amplified negative feedback voltage source by inserting a suitable voltage reference D1 between the emitter of transistor Q1 and resistor R1 (Figure 9). As previously discussed, the voltage reference can be a series of diodes, an LED or a zener diode.

Voltage reference D1 is supplied with a constant current, which is largely immune to supply rail variations, by resistor R1. The voltage output is taken from the emitter of transistor Q1. Resistor R3 increases stability margins of the feedback loop; alternatively, as previously demonstrated, pole-zero shunt compensation from the collector of the control transistor Q2 may be used to accomplish this objective.

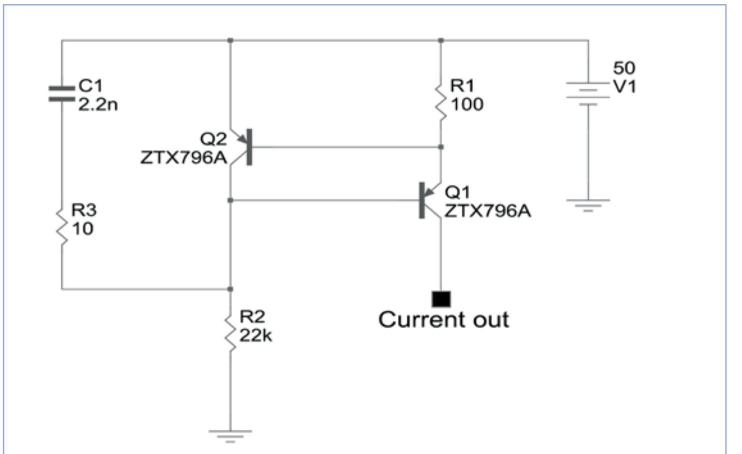

Figure 7: The pole-zero shunt compensation network, comprising R3 and C1, allows relatively accurate placement of the unity loop gain zero

Variation of the ANF voltage source's output impedance with frequency is shown in Figure 10. This plot was obtained by connecting a grounded ideal independent current source to the output of the ANF voltage source and running an AC analysis with respect to the ideal current source. The output impedance is then merely the ratio of the output voltage to the current delivered by the ideal current test source.

The test source needs to be a current source and not a voltage source because the circuit under test is a nominal voltage source which, therefore, requires a test source with an infinite output impedance to prevent erroneous results being obtained due to the loading of the test source on the circuit under test.

The output impedance of the ANF voltage source is inductive, being of the order of tens of milliohms across the audio band before increasing sharply at ultrasonic frequencies (see Figure 10). To prevent this rise in impedance shunt capacitor C1 to ground is connected across the ANF voltage source's output (Figure 9). Shunt capacitor C1 should be at least 47uF to be effective, as Figure 10 reveals. Capacitor C2 prevents power supply ripple from significantly disrupting the feedback loop; in other words, capacitor C2 improves the power supply rejection ratio (PSRR) of the ANF voltage source.

To obtain the circuit's PSRR with frequency, an ideal AC voltage source was connected in series with the DC voltage source V1 energising the circuit. The frequency response (effectively the PSRR) with respect to the output of the ANF voltage source was then obtained (Figure 11). Capacitor C2 improves the PSRR of the ANF voltage source by nearly 50 dB (to over 110dB) at the ripple frequency of 100Hz. The decrease in PSRR beyond 1kHz and with C2 in situ is due to ripple injection through the collector of transistor Q1, while the increase in PSRR beyond 80kHz is due to capacitor C1 shunting the output.

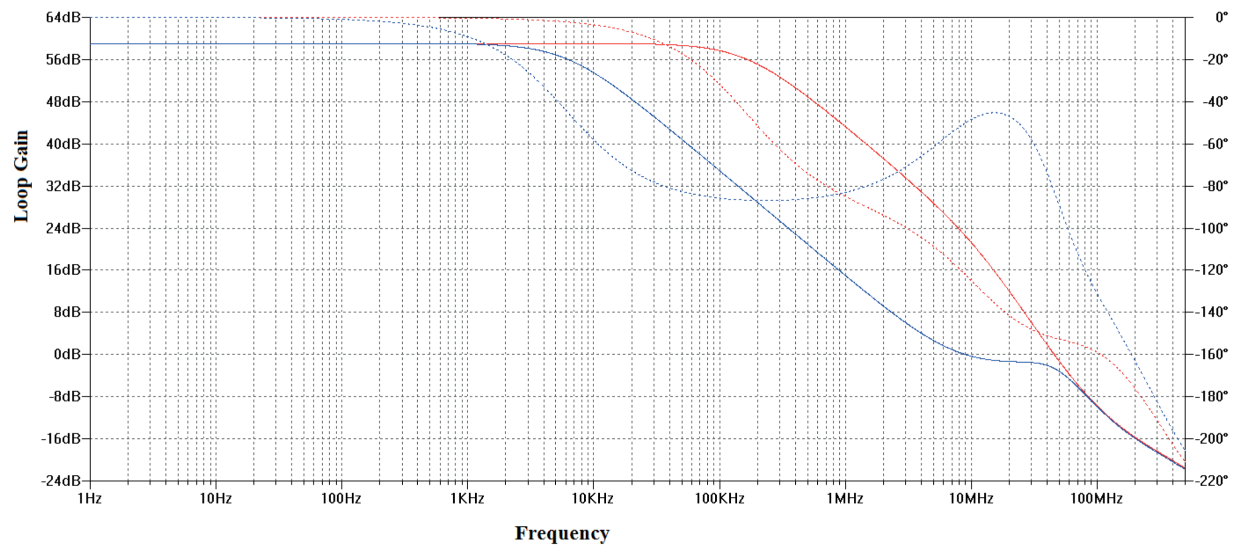

Loop gain without shunt compensation network

Loop gain with shunt compensation network in situ

Figure 8: Shunt compensation network increases phase margin from 28 degrees to 130 degrees

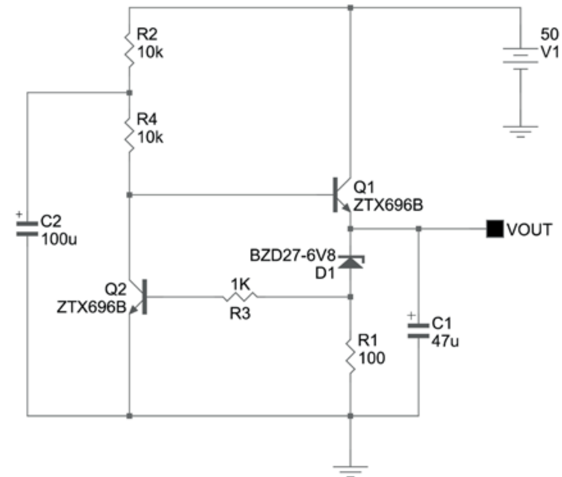

Figure 9: The amplified negative feedback voltage source

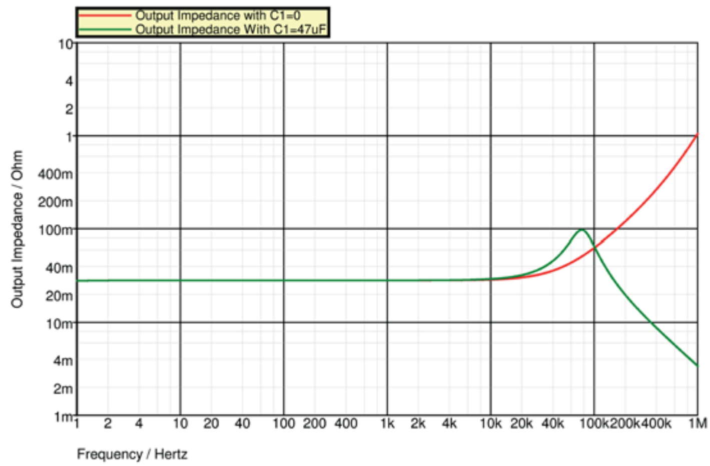

Figure 10: The output impedance of the ANF voltage source is inductive in the absence of output shunt capacitor C1

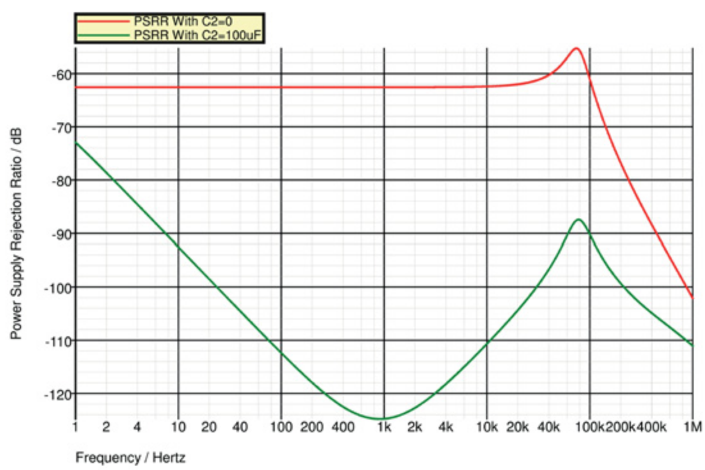

Figure 11: Decoupling capacitor C2 improves PSRR of the ANF voltage source by nearly 50dB (to over 110dB) at the ripple frequency of 100Hz

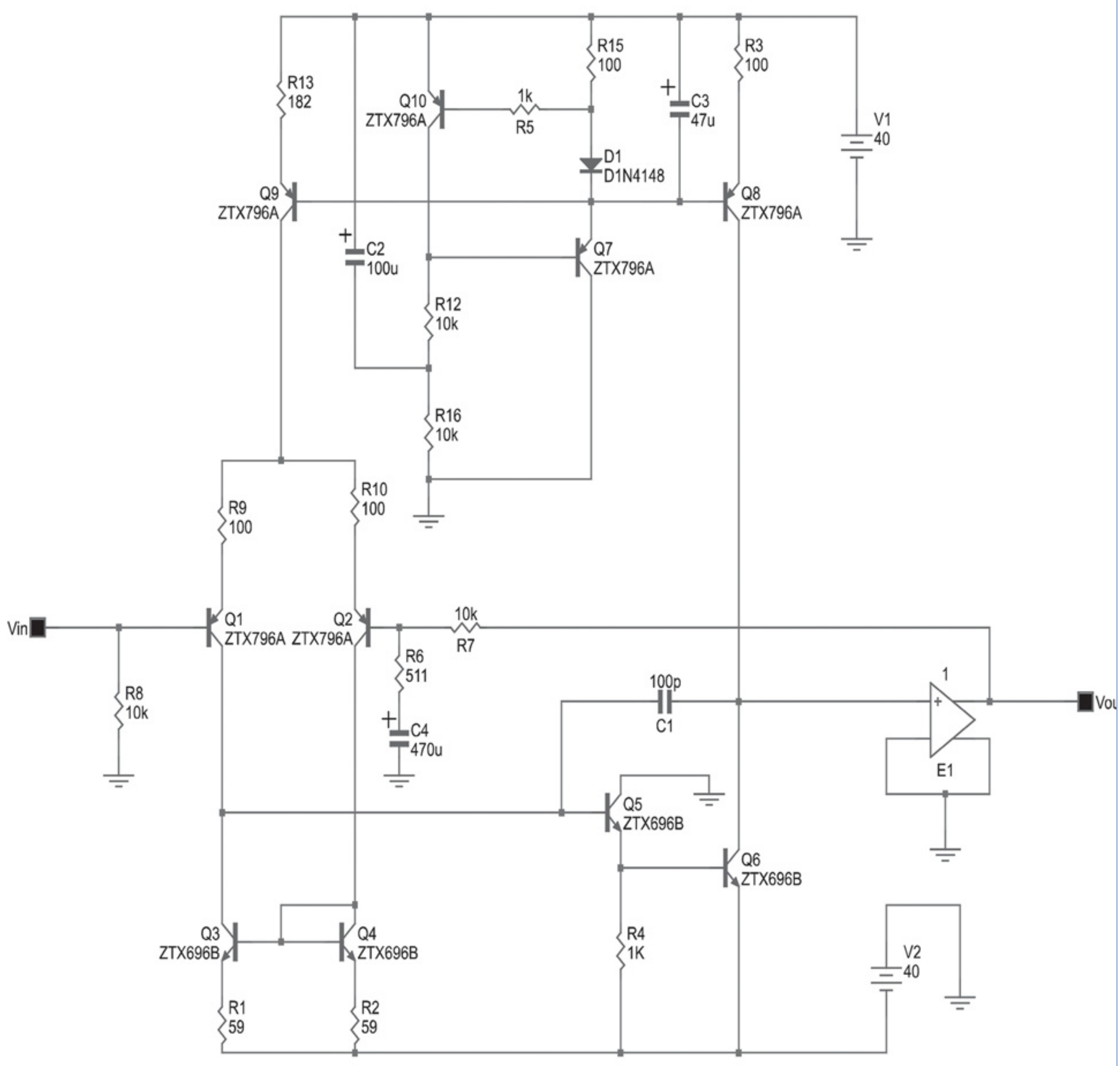

Figure 12: The rudiments of an amplifier of the Thompson topology whose current sources are biased by a single ANF voltage source. The input stage is a transadmittance stage (TAS) while the second stage is a transimpedance stage (TIS); the unity-gain voltage-controlled voltage source E1 represents the output stage of the amplifier

Applications

The ANF voltage source may, for example, be used as a low-impedance voltage source to bias the current sources of the transadmittance stage (TAS) and the transimpedance stage (TIS) in the amplifier of the form shown in Figure 12. This marginally reduces the component count compared with using two separate ANF current sources, but it compromises performance, at least in principle, because, as previously noted, the output impedance of each current source is now less than one tenth, at 100Hz, of that if wholly independent ANF current sources were used to bias the TAS and the TIS.

The ANF current source is a simple and versatile circuit whose output impedance greatly surpasses that of virtually all forms of discrete-transistor voltage-reference-biased current sources across the audio band. In fact, the ANF current source's output impedance is of the same order as that of a cascode current source, with the additional advantage that it functions with a significantly smaller voltage drop across it (compliance voltage) than the cascode current source; it also has a much smaller component count compared with the cascode current source.

The versatility of the ANF current source is underscored by the fact that it can be modified to function as a low-impedance voltage source. Given its low cost, it is difficult to conceive of any reason not to use the ANF current source exclusively where a current source is called for in the design of discrete audio amplifiers. ●


Atlas DCA - Semiconductor Analyser model DCA55
- Connect any way round.
- Automatically identify component type.
- Automatically identify pinouts.
- Supports Transistors, MOSFETs, Diodes, LEDs and more.
- Measure transistor gain (hFE).
- Measure VBE (now 1mV resolution!)
- Measure leakage current.
- Measure MOSFET thresholds.
- Measure LED voltages.
Now with backlit display and AAA battery!
2 Year Warranty as standard
£48.00
(£40.00+VAT)
UK delivery £3.00 inc. VAT
atlas DCA
model DCA55
PEAK electronic design ltd
AAA Battery Edition
Base-Emitter V
VBE=1.039V
semiconductor component analyser
automatic lead identification
on - test
scroll - off
warning: avoid charge/voltages
PNP Germanium Transistor
RED GREEN BLUE Emit Coll Base
Current gain hFE=67
Test current IC=2.50mA
Base-Emitter V VBE=0.293V
Test current IB=4.981mA
Leakage current IC=0.027mA
NPN Silicon Transistor
RED GREEN BLUE Base Emit Coll
Current gain hFE=117
Test current IC=2.50mA
Base-Emitter V VBE=0.711V
Test current IB=4.583mA
Leakage current IC=0.000mA
PNP Darlington Transistor
RED GREEN BLUE Emit Base Coll
Diode protection between C-E
Current gain hFE=9124
Test current IC=2.50mA
Base-Emitter V VBE=1.321V
Test current IB=3.720mA
Leakage current IC=0.000mA
Enhancement mode N-Ch MOSFET
RED GREEN BLUE Gate Drn Srce
Gate Threshold VGS=3.47V
Test current ID=2.50mA
Diode or diode junction(s)
RED GREEN BLUE Anod Cath
Forward voltage VF=0.694V
Test current IF=4.663mA
Three terminal bicolour LED
Pinout for D1
RED GREEN BLUE Anod Cath
Forward voltage D1 VF=1.983V
Test current D1 IF=3.223mA
Pinout for D2
RED GREEN BLUE Anod Cath
Forward voltage D2 VF=1.927V
Test current D2 IF=3.281V
Just a few example screen shots
PEAK® electronic design ltd
Tel. 01298 70012
www.peakelec.co.uk
sales@peakelec.co.uk
E&OE

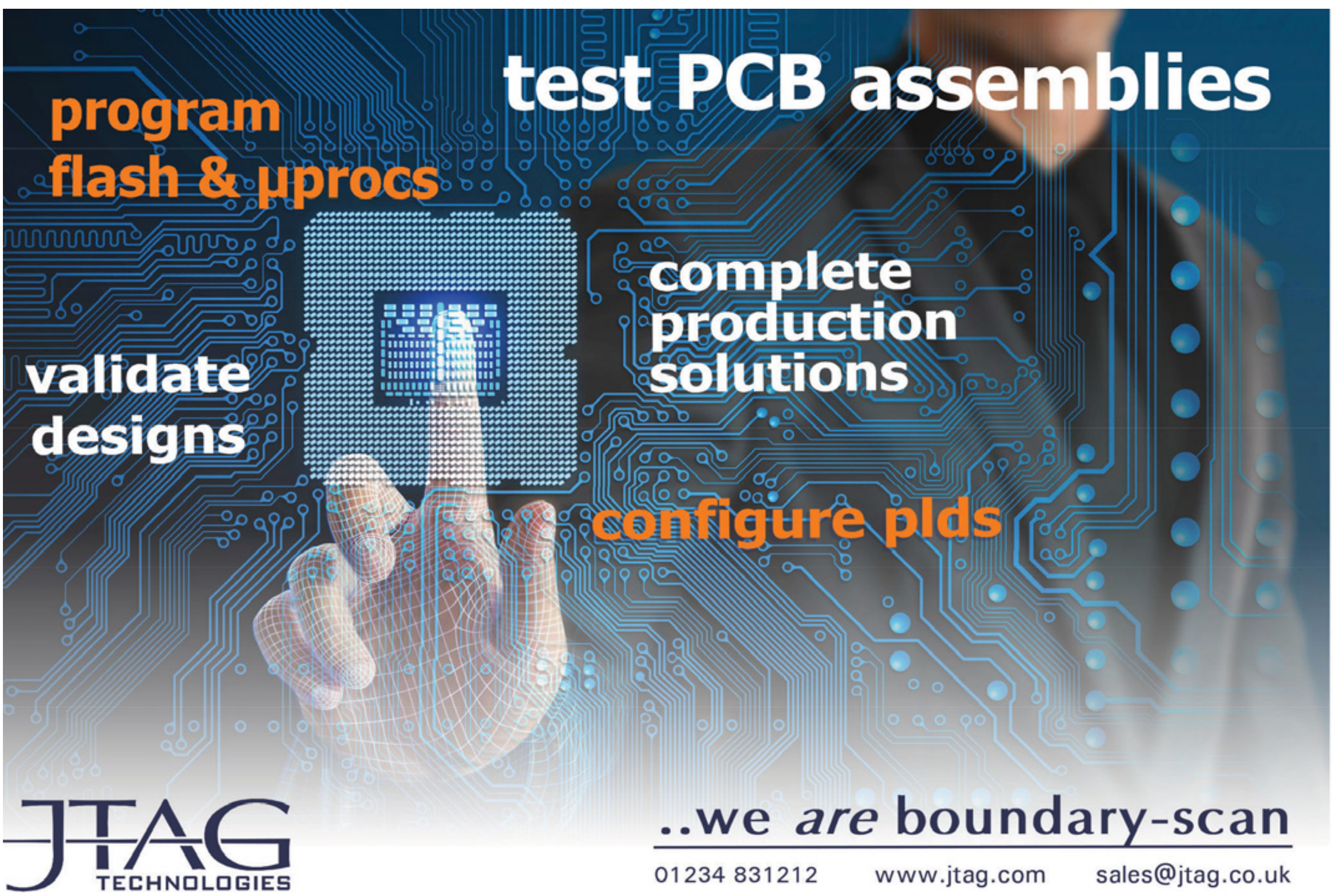
test PCB assemblies
program flash & µprocs
complete production solutions
validate designs
configure plds
JTAG TECHNOLOGIES
..we are boundary-scan
01234 831212
www.jtag.com
sales@jtag.co.uk

LAUNCH OF SCSIFLASH-TAPE PROVIDES SOLID STATE REPLACEMENT FOR OBSOLETE AND END-OF-LIFE TAPE DRIVES

Solid State Disks launched SCSIFlash-Tape which provides a CompactFlash-based, solid state replacement for traditional SCSI-based, electro-mechanical tape drives on legacy computer-based systems that are either obsolete or nearing the end of their life. SCSIFlash-Tape provides a drop-in replacement for the popular DDS DAT, DLT and QIC tape drives on a variety of host systems.

Offering a fast and efficient field replacement, SCSIFlash-Tape's configurable firmware, which is field upgradeable via an integral USB port, facilitates a perfect match to any host computer system. TCP/IP networking via standard RJ45 Ethernet connection is also supported, allowing SCSIFlash-Tape to be connected to any existing local area network for remote configuration, control, diagnostics, backup and restore.

SCSIFlash-Tape only requires a 5V power supply and will also fit into a standard floppy disk drive slot using the same fixings.

www.ssd.gb.com

NEW APPOINTMENT AT EMC, RADIO & SAFETY TEST SERVICE, RN ELECTRONICS

Leading EMC, Radio & Safety Test Service, RN Electronics is delighted to announce the appointment of Paul Ray as Managing Director. Paul joins the family company and takes over the role from Sue Ray. The company began trading in 1987, when, father, Roger Ray left his position as Group Chief of Marconi Mobile Radio to launch the company with his own product range and RF design service. Roger and Sue have grown the company over the 30 years, Roger Ray remains actively involved as Technical Director.

Paul Ray brings with him experience and knowledge of industry, having worked as a Purchasing Manager in pharmaceuticals and medical devices. He will play a key role in managing the company's ongoing expansion and growth goals as well as building on the firm's outstanding reputation for service and delivery to professional clients.

www.rnelectronics.com

VERSASENSE PRESENTS MICROPNP PLUG-AND-PLAY IOT PLATFORM

VersaSense will present live demonstrations of its award-winning MicroPnP product range at Electronica, on the Linear Technology stand 524, hall A4. MicroPnP is the standards-compliant and low-power Sensing-as-a-Service solution that combines zero-configuration plug-and-play integration of IoT peripherals, scalable and 24/7 monitoring and control of devices across different sites, with secure and ultra-reliable wireless networking from Linear Technology.

The MicroPnP platform offers a complete hardware and software platform supporting a range of over 50 different plug-and-play sensors. MicroPnP features a unique value proposition by enabling true plug-and-play identification and integration of any sensor and actuator at 10 million times lower power than existing solutions; it offers ultra-reliable networking through SmartMesh IP from Linear Technology (> 99.999% end-to-end data reliability) and its next-generation security techniques guarantee security and privacy from the embedded sensor to the cloud.

www.versasense.com
www.linear.com

NEW AUTOMOTIVE MULTI-OUTPUT POWER MANAGEMENT IC FROM ALLEGRO

Allegro MicroSystems Europe has announced a new power management IC that can be configured as a buck or buck-boost pre-regulator to efficiently convert automotive battery voltages into a tightly regulated intermediate voltage complete with control, diagnostics and protections. The output of Allegro's A4413 supplies both a 5V, 75mA maximum high-voltage protected low drop-out (LDO) regulator for remote sensors, and a 0.8-3.3V, 800mA maximum adjustable synchronous buck regulator (ADJ). Designed to supply microprocessor power supplies in high-temperature environments, the device is ideal for under-hood and other automotive applications.

The A4413 can be enabled by its logic-level input (ENB) or its high-voltage input (ENBAT). Diagnostic outputs from the new device include a power-on-reset output with a 2ms rising delay to monitor the synchronous buck, a power OK output to monitor the 5V LDO, and an ENBAT status output (ENBATS).

www.allegromicro.com

EMBEDDED DESIGN SHOW — WWW.ENGINEERING-DESIGN-SHOW.CO.UK

Harmonic

Would you benefit from :

On site expertise to get your projects back on track?

Agile Engineering Services for VxWorks and Embedded Linux?

Years of experience with multiprocessing, hypervisors, hardware virtualization, networking, device drivers and board support packages?

Embedded Security for your next IoT device?

Customer Testimonial:
"Their knowledge of the Wind River tools and VxWorks RTOS was phenomenal. This combined with their structured approach to fault isolation and processor knowledge made their efforts invaluable to us."

Contact: Visit us at stand G35,
Embedded Design Show,
19TH-20TH October,
Ricoh Arena, Coventry
www.harmonicss.co.uk
sales@harmonicss.co.uk
01403 784500

Stand: G35

EMBEDDED DESIGN SHOW — WWW.ENGINEERING-DESIGN-SHOW.CO.UK

Geyer

Geyer Electronic eK was founded in 1964, selling electronic components from a small office in central Munich. 50 years on and Geyer is now well known as a manufacturer and supplier of high quality Frequency Control Products for the Automotive, Telecom, Medical and Security, Consumer/Multimedia and Industrial Electronics. With an international network of Sales Offices and distributors, factories in Taiwan, Japan and S Korean, and a Design and Test Center at its Headquarters in Germany, Geyer Electronic is able to offer dedicated support to their clients from design stage, through to volume production, manufacturing around 75 million parts per month to IS09001, ISO 14001 and TS15949/AEC-Q200 standards

Geyer eK moved to their Headquarters in Gräfelfing, in the west of Munich, in 2002 where they were able to benefit from the access offered by the Autobahn routes, and opened a Design and Test Center in 2011 to develop the crystal products and to work with clients on custom-designed solutions for their applications. Since that time, the Design Center has been expanded and now offers a comprehensive consultation service from our team of five Application Engineers, providing design validation, custom samples and prototype devices, and 3D models of our components to help customers' engineers during the design stages. We also offer the unique Y-Quartz App to help Design Engineers select the optimum crystal specifications to work in their system, supported by advice from our Application Engineers if requested.

Geyer Electronic UK Ltd, based at their office in Romsey Hampshire, supports customers in the UK and Ireland by working closely with their R&D teams, using the Munich sales support and Design Centre to help identify the optimum crystal, oscillator, SAW filter or resonator for their projects and supplying samples for evaluation and prototype builds.

Contact: sales@geyer-electronic.co.uk
or by phone on +44 (0)1794 329341

Stand: J6

EMBEDDED DESIGN SHOW — WWW.ENGINEERING-DESIGN-SHOW.CO.UK

Euroquartz

Euroquartz is the sole remaining UK quartz crystal manufacturer of high specification HC49U, UM1 and UM5 crystals, as well as a range of military clock oscillators and crystal filters.

Manufacturing, engineering and sales are situated in a custom-built modern facility in Crewkerne, Somerset, UK from where a comprehensive range of frequency control products is also offered. The recently upgraded facility enables Euroquartz to perform full military screening tests and qualification testing on all other products in the company's portfolio.

The test capabilities of the facility include accurate frequency measurement, temperature cycling, acceleration testing, gross leak, fine leak, filter characteristic testing as well as active burn-in routines. Custom crystal selection testing is also offered from the Euroquartz test facility.

Founded in 1982, the company has a wealth of experience and technical knowledge making it a leading specialist in the field of frequency products. Customer service and quality are the main driving forces behind the business, a fact clearly demonstrated by the company's AS9100 quality certification awarded in 2015.

As a long-standing and well respected manufacturer in its own right, Euroquartz has access to many very specialised sources of supply that are not available from many of their competitors.

Euroquartz is a privately owned British-company providing a flexible and quality service unrivalled in the frequency control field.

Contact: Tel: +44 (0)1460 230000
info@euroquartz.co.uk

Stand: F2

EUROPEAN MICROWAVE WEEK — WWW.EUMWEEK.COM

Electro Rent

Since 1965, Electro Rent has been giving its customers alternative ways to acquire, implement and manage their test equipment resources. The company provides flexible equipment rental and leasing, new and used sales, and full service solutions. By offering this range of services Electro Rent ensures that its customers can get the equipment they need, when they need it and at a cost that's within their budget.

The inventory includes a comprehensive range of RF/Microwave, Power Systems, Communications and General Purpose test equipment used by companies operating in the aerospace and defense, semiconductor, telecommunications and electronics industries.

Electro Rent can supply equipment from over 200 suppliers, and has longstanding relationships with all of the major test equipment manufacturers, particularly because it buys its inventory pool new from those manufacturers. The company has the largest inventory of test equipment in the world and all of this equipment can be supplied on a rental or leasing basis. In addition because the inventory is turned over regularly there is always a selection of ex-inventory used equipment available for sale.

Electro Rent's global network of dedicated account managers and professional business specialists help you plan your procurement strategy. Internal technical professionals handle all requests efficiently and risk free: quote requests, availability, fast delivery and more.

Contact: www.electrorent.co.uk • sales.uk@electrorent.com

Electro Rent EUROPE
An Electro Rent Global Company

Stand: 171

ELECTRONICA — WWW.ELECTRONICA.DE

ODU: not your average connector company

As a problem-solving connector manufacturer, ODU enjoys single-source status with over one hundred of the world's top manufacturing companies. Why is that? Because, not only does it have expertise, but it works hard at being a flexible and innovative supplier.

In the UK, ODU is probably best known for its miniature military push-pull connectors.

Notably, since 2002, ODU has supplied more than 100,000 helmet connectors for use on the UK Bowman military communications programme, without a single reported connector failure.

The AMC (Advanced Military Connector) series was originally developed to meet the ever-demanding needs of the many international 'Future Soldier' programmes, intended to equip the average ground-based combat soldier with an integrated set of high-technology systems, linked to an array of battlefield information resources.

Now this range of rugged connectors has been expanded to offer high-performance data transmission, high bandwidth, high reliability and easy handling in any harsh environment and in sizes that are typically a third smaller and lighter than MIL-Std housings.

The AMC range includes numerous high-density signal configurations, with transfer rates up to 10Gbit, and versions for combined signal and power up to 15A, in a compact package.

Performance characteristics include 5,000 mating cycles, push-pull or break-away functions for maximum safety, watertight to IP68/IP69, optimised mechanical and colour coding, highly reliable 360° shielding, operating temperature of -51°C to +125°C, salt spray resistance and so on.

ODU will be at several exhibitions this year so, if you are faced with a connector or packaging problem, then why not come and talk to its representatives, or get in touch now:

Contact: miniaturemilitaryconnectors.co.uk

ODU®
A PERFECT ALLIANCE.

Hall: B2
Stand: 143

ELECTRONICA — WWW.ELECTRONICA.DE

Apacer: the most reliable storage for industrial and embedded applications

Apacer Technology Inc was founded in 1997 in Taiwan and positioned itself to be an agile supplier of DRAM whose primary operations focused on memory modules. By 1999 Apacer had become the world's fourth largest memory module manufacturer.

With an optimistic view on the flash market and as a response to the changes in the memory industry, Apacer developed its industrial memory line in the early years of 2000.

Today, Apacer offers a large portfolio of innovative Solid State Drive Solutions (SATA, PATA, Flash Cards and USB) and DRAM Solutions (desktop, notebook and server) for the industrial and embedded markets. More recently, Apacer developed a range of data security technologies by launching data security enhanced products and unique value added features.

One of our strengths lies in its customization capabilities: its industrial SSD line offers a wide range of different specifications in terms of size, angle, thickness and functions such as high capacities with strong performance, wide temperature support and shock- and vibration resistance for various industries: military, aerospace, networking, medical, automation, gaming etc.

Apacer's DRAM module technology development is focused on vertically integrating know-how in the semiconductor industry, manufacturing memory modules that satisfy the requirements of quality, performance and, yet, can be easily integrated into various platforms.

Contact: eu.apacer.com

Apacer

Hall: A6
Stand: 439


DO YOU WANT THE BEST
ELECTRONICS DESIGN SOFTWARE?
PROTEUS
The Alternatives
User Friendly
Comprehensive
Integrated
Affordable
Danger
FEATURES
• Schematic Capture
• PCB Layout
• Gridless Autorouting
• 3D Visualization
• M-CAD Integration
• SPICE Simulation
• MCU Co-simulation
• Built in IDE
• Visual Programming
Labcenter
Electronics
www.labcenter.com
Tel: +44 (0)1756 753440